

**Engineering and Architecture School.**

**Electronic Engineering.**

Electronic and Communications Science and Technology Master  
Program.

**Master Thesis**

On

Hardware-software Embedded Systems.

**Online Alpha Wave detector: An Embedded hardware-software  
implementation.**

**Candidate.**

**Victor Javier Kartsch Morinigo.**

**Supervisor.**

**Chiar.mo Prof. Luca Benini.**

**Co-supervisor.**

**Dr. Simone Benatti.**

**Academic Year 2015/2016.**

**Session II.**

## **Abstract**

The recent trend on embedded system development opens a new prospect for applications that in the past were not possible. The eye tracking for sleep and fatigue detection has become an important and useful application in industrial and automotive scenarios since fatigue is one of the most prevalent causes of earth-moving equipment accidents. Typical applications such as cameras, accelerometers and dermal analyzers are present on the market but have some inconvenient. This thesis project has used EEG signal, particularly, alpha waves, to overcome them by using an embedded software-hardware implementation to detect these signals in real time.



# Index.

<b>1. Introduction.</b>	<b>Pg.1.</b>
<b>2. Electrophysiology, the body signals.</b>	<b>Pg. 6.</b>
2.1 Classification of Bio-signals.	Pg. 8.
2.1.1 EMG (Electromyography) Signals.	Pg. 8.
2.1.2 ECG signals (Electrocardiography).	Pg. 9.
2.1.3 EEG signals (Electroencephalography).	Pg. 11.
2.2 The Alpha Waves.	Pg. 13
2.3 Extraction of the signals.	Pg. 13
2.4 Inconveniences when working with EEG signals.	Pg. 16.
2.4.1 External interference.	Pg. 16.
2.4.2 Internal interference.	Pg. 17.
<b>3. EEG Board, design and features for the project.</b>	<b>Pg. 21.</b>
3.1 EEG board Hardware Scheme.	Pg. 22.
3.1.1 The ADS1298.	Pg. 22.
3.1.2 STM32F407VGT6 microcontroller	Pg. 23.
3.1.3 Pressure and accelerometer.	Pg. 24.
3.1.4 Bluetooth Transcriber.	Pg. 24.
3.2 Working Principle.	Pg. 25.
3.3 Firmware architecture.	Pg. 26.
<b>4. Android application.</b>	<b>Pg. 29.</b>
4.1 Main parts and working principle.	Pg. 29
4.2 Steps for the reception of the values form the microcontroller.	Pg. 31.
4.2.1 Bluetooth Connection.	Pg. 31.
4.2.2 Application Tasks.	Pg. 32.
4.3 Modification for evaluation of the final performance.	Pg. 33.
<b>5. Data Collection and modeling on Matlab.</b>	<b>Pg. 35.</b>
5.1 Data Collection.	Pg. 35.
5.2 Establishing metrics for determining the performance.	Pg 37.
5.3 Threshold Based approaches.	Pg. 38.
5.3.1 Threshold using PSD.	Pg. 38.
5.3.2 Threshold using an envelope approach.	Pg. 41.

5.4	Decision Tree based approaches.	Pg. 46.
5.4.1	Binary Decision Tree.	Pg. 46.
5.4.2	Binary Decision Tree including the PSD as a feature.	Pg. 48.
5.4.3	3-Ary Decision Tree.	Pg. 48.
5.4.4	Blink trained as 'open eyes'	Pg. 49
5.5	Data analysis and selection of the final Implementation.	Pg. 50.

**6. Implementation of the model and experimental results. Pg. 52.**

6.1	Translating the code to C.	Pg. 52.
6.2	Other adaptations of the code.	Pg. 54.
6.3	Testing Setup.	Pg. 56
6.4	Results.	Pg. 57.

**7. Conclusions. Pg. 59.**

**Acknowledgements Pg. 60.**

**Bibliography Pg. 61.**

## Summary of the figures.

**Figure 1.** *AntiSleep by SmartEye.*

**Figure 2.** *Muse Neuro Feedback.*

**Figure 3.** *Development process of the Alpha wave detector.*

**Figure 4.** *System for bio-potential extraction.*

**Figure 5.** *EMG signal generation.*

**Figure 6.** *Electrode's configuration for EMG.*

**Figure 7.** *EMG signal*

**Figure 8.** *Myo Gesture Control.*

**Figure 9.** *ECG signal.*

**Figure 10.** *International 10-20 reference system for EEGs.*

**Figure 11.** *Alpha waves after filtering.*

**Figure 12.** *Alpha waves electrode location.*

**Figure 13.** *Covidien Electrodes used on this work.*

**Figure 14.** *Notch Filtered signal.*

**Figure 15.** *Eye blink artifacts on EEG.*

**Figure 16.** *Artifacts on the spectrogram of the signal.*

**Figure 17.** *EMG artifacts.*

**Figure 18.** *Electrode slicing artifact.*

**Figure 19.** *Ground Lead off artifact.*

**Figure 20.** *Pipeline for extraction of EEG signals.*

**Figure 21.** *The ADS1298.*

**Figure 22.** *STM32F407 Block diagram.*

**Figure 23.** *Other modules of the EEG board.*

**Figure 24.** *Working principle of the board.*

**Figure 25.** *EEG Board PCB.*

**Figure 26.** *State Machine on the microcontroller.*

**Figure 27.** *Android EEG Reader.*

**Figure 28.** *Visualization Screen and options on Android EEG Reader.*

**Figure 29.** *Bluetooth connection pipeline.*

**Figure 30.** *Application flow diagram.*

**Figure 31.** *Implemented application.*

**Figure 32.** *Test mode of the EEG Signal manager.*

**Figure 33.** *EEG signal extracted using the EEG Board.*

**Figure 34.** *Spectrogram of the extracted data.*

**Figure 35.** *Confusion matrix example.*

**Figure 36.** PSD Threshold algorithm.

**Figure 37.** PSD threshold detector implemented in one trial.

**Figure 38.** Magnitude Response of different filters.

**Figure 39.** Filtering process.

**Figure 40.** Smoothing of the envelope using different values of the window.

**Figure 41.** Envelope approach algorithm flowchart.

**Figure 42.** One trial with Threshold using an Envelope approach.

**Figure 43.** Decision Tree example.

**Figure 44.** Binary decision tree predictions

**Figure 45.** Binary decision tree predictions after eliminating some features.

**Figure 46.** 3-ary Decision tree with PSD model prediction using blink as a new class.

**Figure 47.** Blink trained as 'open eyes' model prediction.

**Figure 48.** Performance graph.

**Figure 49.** Final model.

**Figure 50.** CMSIS Library Scheme.

**Figure 51.** Circular Buffer.

**Figure 52.** Decrease of the Alpha waves signal amplitude.

**Figure 53.** Algorithm used for the adaptations.

**Figure 54.** Test phase

**Figure 55.** Testing application showing test process and results.

## Summary of the Tables.

**Table 1.** *Brain Waves (or rhythms).*

**Table 2.** *PSD threshold comparison.*

**Table 3.** *PSD threshold comparison.*

**Table 4.** *Envelope threshold comparison.*

**Table 5.** *Envelope threshold comparison.*

**Table 6.** *Binary decision tree model comparison.*

**Table 7.** *Binary decision tree eliminating some features.*

**Table 8.** *Decision tree with PSD model comparison.*

**Table 9.** *3-ary Decision tree with PSD model comparison using blink as a new class.*

**Table 10.** *Decision tree with Blink as Open eyes.*





# 1. Introduction

The recent trend on embedded system development opens a new prospect for applications that in the past were not possible. Thanks to this, nowadays is possible to find solutions that combine energy efficiency and processing capabilities. Activity recognition and HMI (Human Machine Interaction) take advantage from this technological boost to become more pervasive in many daily living applications enabling assistive solutions to improve quality of life and safety.

During the last years, the eye tracking for sleep and fatigue detection has become an important and useful application in industrial and automotive scenarios. According to a report by Caterpillar [1], the world's largest manufacturer of construction and mining equipment operator, fatigue is one of the most prevalent causes of earth-moving equipment accidents (large vehicles such as bulldozers and excavators) within the mining industry. The shifts of the workers can often be 12-hours long, which creates the risk of "micro-sleeps" when suffering from fatigue, that can, in turn, compromise the safety of the workers and the operations. This also applies for other areas like long tour bus, trains, planes and car driving jobs.

To cope with these issues, automotive industry started to study eye tracking systems that monitor the position of the driver's eyes, count the eye blink ratio and detect when there is suspect of a sudden-onset sleep. One example of this is the 'Attention Assist', a systems developed by Mercedes-Benz which warns the driver of their level of fatigue and how much time has passed since their last break from driving [2]. Also, it's possible to find on the market some wearable devices like the Anti-Sleep Alarm, that works by scanning the electrodermal activity to determine if the user is falling asleep or if the reaction capability has decreased. Another implementation relies on accelerometers. In this case, depending on the inclination of the head the system will trigger an alarm. Other applications are based in camera technology, like that case of Micro-Sleep Tracker and Eyetracker, developed by the Fraunhofer Institute for Digital Media Technology IDMT in Germany, a two camera and control unit solution that tracks the position of the eyes [3]. Also, following the same principle, it's possible to find the AntiSleep, a device developed by Smart Eye, a company that created a compact one-camera solution that is specially designed for automotive in-cabin real-time measurements of the driver head pose, gaze direction and eyelid closure [4].



*Figure 1. AntiSleep by SmartEye [4].*

The methods above have still some constrain attached to their working principle. In the case of the cameras, the devices require to have a clear line of sight (i.e., avoiding the use of glasses or some other obstructions) and good alignment, the accelerometers require a stable position of the head and dermal detection systems may have a lag of time while processing the signals. All these conditions affect their robustness and make them prone to missed detections and false alarms.

An alternative method is found through the analysis of the brain activity. The Brain Computer Interface (BCI) is an interface that allows the extraction of EEG (Electroencephalography) signals, i.e., the brain signals. Currently, the BCIs are used for brain mapping, neural prostheses control and also for the detection of pathologies like epilepsy [5]. Thanks to the use of Brain Computer Interfaces (BCIs) it's possible to extract some features in order to detect the closure of the eyes.

Initially, the acquisition of information on the brain activity was done using computer based BCIs, since the analysis of the information require high computational power that was not available on embedded systems at that time. Currently is possible to find many researches and development of systems that can use innovative embedded devices. The detection and characterization of the signals are done using DSP techniques and the optimization of the algorithms that allow them is strongly studied to find the best model that can increase the accuracy of the predictions.

Regarding the EEG signals, they can be classified depending on the frequency band in which they appear since each band may have a different meaning in terms of the processes that

trigger them. One of this frequency bands correspond to the *Alpha waves* that are mostly generated from the occipital lobe of the brain. They are originated during awake relaxation with closed eyes, in which relies the working principle of the implementation of this thesis project.

The analysis of EEG signals can be challenging due the particular properties of the signal on itself and the interference to which they may be subject to. Nevertheless, it's possible to find on the market embedded that can perform some analysis, especially for neurofeedback like the Muse Neuro Feedback, used in meditation.



*Figure 2. Muse Neuro Feedback [6].*

Particularly on the field of alpha wave detection, some work has been done recently, mostly promoted by the OpenBCI board, an open source EEG reader. This board has the capability to sample the signals coming from the brain and stream the data to a serial port. Using this board, The OpenBCI Alpha Wave Detector project has achieved good results using energy detection [7].

This work relies also on the detection of the Alpha waves in order to determine the condition of the eyes of the user. The main goal is to develop an Embedded hardware-software application able to generate an output that can be used to trigger alarms in real time detecting these Alpha waves. Since several DSP techniques are available for this task, the evaluation of the performance with the different approaches became an important part for the project. Also, some disadvantages had been overcome since working with EEG signals can be highly challenging.

We started by developing a board that could be able to extract information from the brain signals using a powerful ADC converter, the ADS1398 in conjunction with a Cortex M4 based STM32F4 microprocessor, responsible for acquire the information from the ADC, do the signal processing required and finally stream the data to an Android device in order to visualize the outputs.

Initially, some offline data acquisition was performed in order to model the final system. For doing it so, the hardware mentioned above was used just to collect raw data from various test subjects and various trials. This required some minimal programming on the microcontroller and the development of an Android application that can capture this data and then make it available for its analysis using Matlab.

After the modeling on Matlab, having tested different approaches for the detection, the method that gave good accuracy and had a simple operation was selected for the implementation on the microcontroller. The scripts had been translated to C programming language and adapted to be used with real time data. Also, the android application had been changed to a more suitable interface that can register and show the result of the tests. In the following figure is possible to see a pipeline that group all development process.

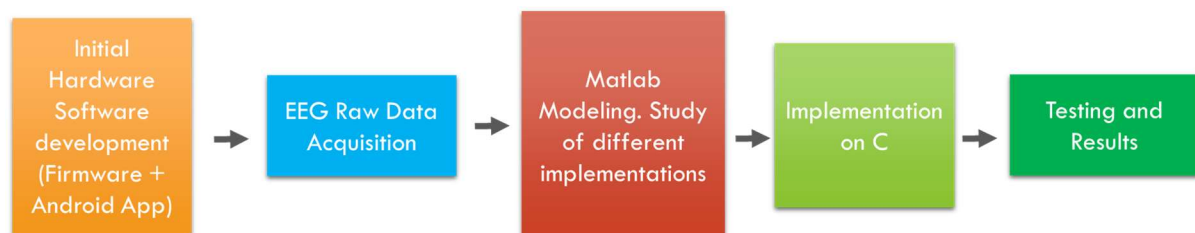


*Figure 3. Development process of the Alpha wave detector.*

In the following pages, specific information about the mentioned steps will be provided, classified in the subsequent list:

- **Electrophysiology, the body signals:** In this chapter, a theoretical frame will be exposed, that concerns to the signals that the body, in general, can generate, taking special emphasis on the EEG signals and the techniques for the detection.
- **EEG Board, design and features for the project:** the main concepts about the integration of the different devices will be mentioned, starting from the design of the board

and its motivation, the capabilities and the firmware used for a basic working for streaming raw data.

- **Android application:** this chapter, divided in two parts, explains the working principle of the application. The first part concerns to the basic reading of the raw data for the Matlab modeling. The second part describe the changes made in order to have a testing scheme for the final firmware.
- **Data Collection and modeling on Matlab:** a detailed picture of the analysis of the extracted data, modeling of the diverse methods for detection and results will be given. This step was very important since It gave an indication of the best candidate for the final implementation, i.e., for translating to a C programming language afterwards.
- **Implementation of the model and experimental results:** the final implementation is presented with emphasis on the particular requirements for online data as the same as the results obtained with the test subjects using the implementation presented in the previous chapters.

## 2. Electrophysiology, the body signals.

The regular activities of a human are generated by the interaction of different system on the body. The muscles are structures that can execute movement on parts of the body which, instead, are controlled by some signals coming from the brain. At the same time, the generation of movement on itself by these control signals will generate other detectable signals. The latter, in general, is the result of the interaction of particular types of cell that by superposition generate perceptible electric features. The study of the electrical properties of these signals is called Electrophysiology.

The first studies were performed by Galvani 200 years ago, and since this, the technology for reading these signals have changed in a big manner. It has been discovered that by studying them, is possible to detect anomalies on the human body as the same as detecting patterns that can permit the control of prosthetic devices.

The EMG signals (Electromyography), produced by the muscles cells are one these electrical bio-signals. Other kind of signals are, to mention, the ECG signals (Electrocardiography) which consist on the signals generated by the heart muscle, the EOG (Electrooculography) signals, generated by the muscles of the eyes, and some others, that will be expanded in the following pages.

All these signals are relatively easy to detect since they're strong, meaning that they may be on the order of the mVs (millivolts) which gives a better SNR (Signal to noise Ratio) in comparison with some other kind of signal like EEG signals with signals of the order of the  $\mu$ Vs (microvolts).

Particularly, the non-invasive EEG signals (Electroencephalography), that consist on electrical signals coming from the scalp and generated by the brain, as a result of the interaction of neurons, are more difficult to target due the noise and interference by superposition with other signals also generated in the brain (in the case of being targeting a particular brain signal). There exist also an intracranial EEG, which result easier to identify since its lack of external noise but having the problem being an invasive method. For that reason, the non-invasive EEG signals are the ones that result more practical.

In order to extract the bio-signals, a system for this purpose it's required. A typical system can be summarized in the figure 4. The element that is in contact with the tissue, the transductor,

is responsible to transfer the voltage from the subject to the rest of the system. A correct coupling with the tissue is important since it will allow the correct acquisition of the bio-potentials. An incorrect coupling may lead to noisy or unrepeatable measurements. Luckily, most systems have the ability to measure the impedance between them in order to take some corrective actions.

After the transducer, it's possible to find the Analog Front End (AFE). This system is responsible for capturing the incoming signals. It contains a series of conditioning analog circuitry (operational and differential amplifiers mostly) that amplifies and condition the incoming signal providing the desired output for a latter sampling by the Analog-to-digital Converter (ADC). Regarding the ADC, this device is responsible to quantify the values of the sampled instances for a latter signal processing.

The computational block consists in a system that can execute some operations with the values captured by the ADC. The operations can be adjusted according the required output. In the case of bio signals, a typical DSP task will be the addition of filters for eliminating the DC offset on a given measurement or to eliminate some stationary noise, like 50/60 Hz signal precedent from the power supply lines. The analysis of the received information is done also on this block. In this work, one example can be the detection of the alpha waves on itself, which is performed after the filtering a threshold comparison, as it will be explained in the following chapters.

The final block constitutes the outputs of the system that give an indication of the readings or the result of the data analysis. They can be of various kinds. In this project, an Android-based tablet was used for this purpose.

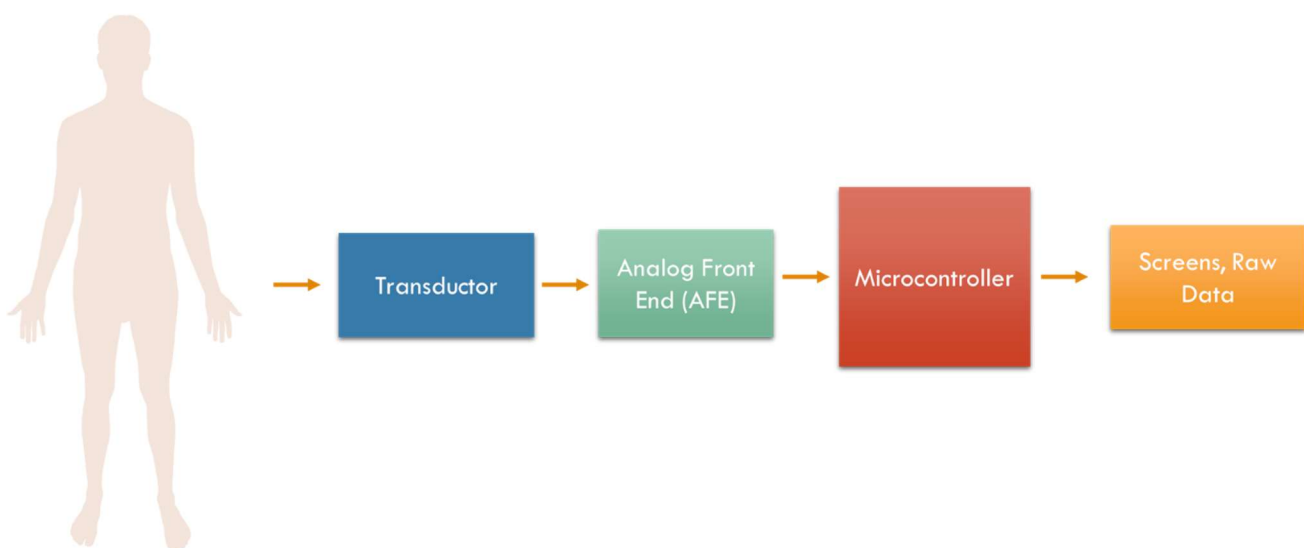


**Figure 4.** System for bio-potential extraction.



## 2.1 Classification of Bio-signals.

As stated before, the bio signals can be classified according the structure that generates the detectable electrical variations. As an extension, the following list summarizes and complement the concepts introduced below:

**2.1.1 EMG (Electromyography) Signals:** these are signals generated by the contraction of the body muscles. Consist in a summation of the electrical activity of the all the muscle cells involved meaning that the size of the muscle will increment the amplitude of the signal. The EMG is generated when a motor neuron action potential from the spinal cord arrives at ta motor end plate. Its arrival causes a release of ACh (Acetylcholine) at the synaptic cleft, which causes a depolarization. This action potential electrically travels downward from the surface in a transverse tubule. This in turn causes a release of  $Ca^{++}$ , causing cross-bridge binding and the sarcomere of the muscle to contract [8].

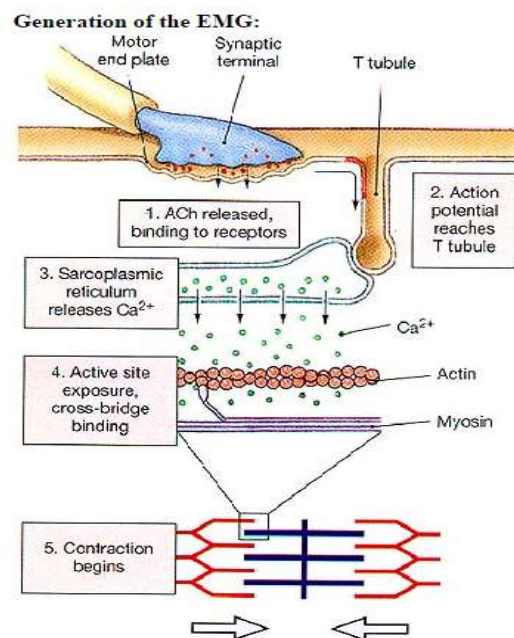
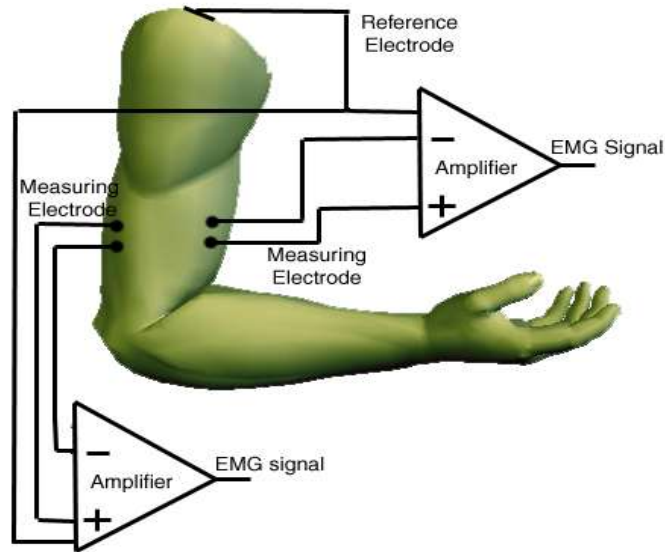


Figure 5. EMG signal generation [8].

The extraction of the EMG signals is done using a series of electrodes that can collect the signal placed at the vicinity of the muscle and a reference electrode which is apart from the ones mentioned before in order to generate the potential difference.



**Figure 6.** Electrode's configuration for EMG [8].

Nowadays, the detection and characterization of these signals are done using signal processing techniques and the optimization of the algorithms that allow them is studied in order to improve the accuracy of the predictions, especially while dealing with prosthetic devices.

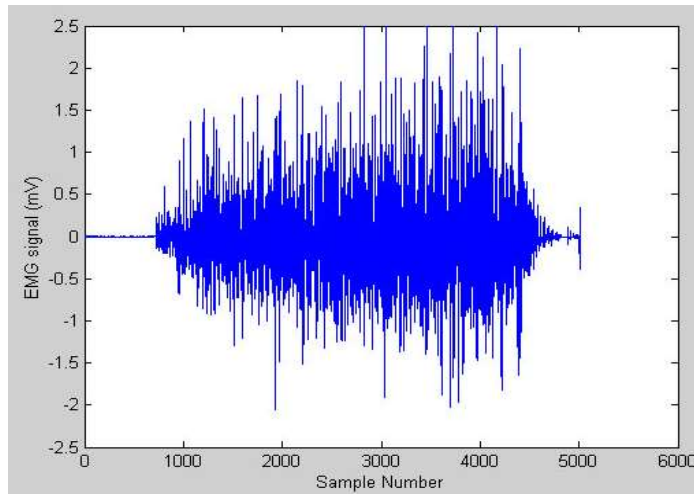


**Figure 7.** EMG signal [8].

Thanks to this, commercial solutions are already present for detecting and transmitting wirelessly EMG signals from hand and arm movements, like the armband developed by Myo, that captures EMG signals to process them into a computer to perform some customizable tasks [9].



*Figure 8. Myo Gesture Control [9].*

2.1.2 **ECG signals (Electrocardiography):** The ECG signals are the result of the depolarization process that occurs during the contraction of the hearth muscle. This electric signal, as the same as the other body signals, is collected at the skin of the subject by the use of electrodes at the vicinity of the hearth. The shape of the signal (One hearth beat) is shown at the Figure 9.

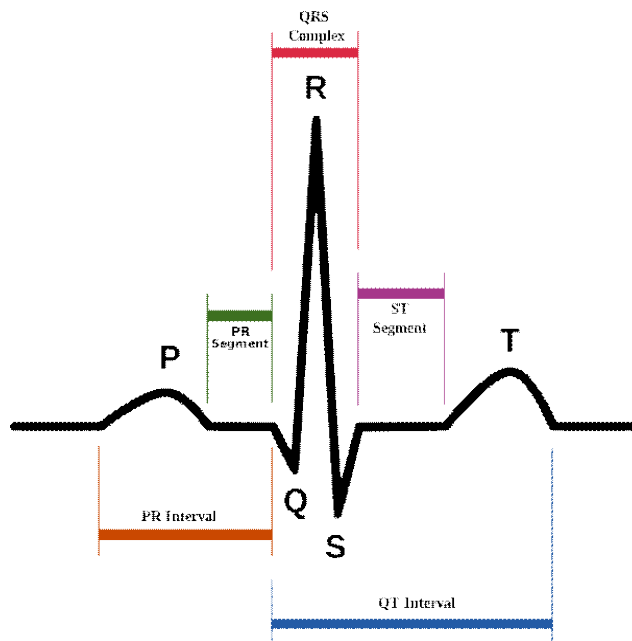


*Figure 9. ECG signal [10].*

The analysis of the ECG signals can vary from calculations of the hearth beat rate to the detection of some pathologies. The intervals that can be seen at the figure are parameters that can give some indications for cardiac disorders.

2.1.3 **EEG signals (Electroencephalography):** These signals result from the interaction of brain cells (neurons). The mechanism from which they're generated relies on the fact that these neurons are polarized by membrane-transport-proteins that pump ions across the membranes. The polarization of the membranes causes a wave effect on the vicinity of the initial ionization that can travel through the brain tissues to the electrodes. Once this wave of ions reaches the electrodes, some electrical charges can be push or pulled generating the voltage variations read by the instruments. The EEG signals are finally the result of the summation of the different neuron contributions, which indicate that the final wave is the result of millions of neurons that have the same spatial ionic orientation. Indeed, one square millimeter of cortex has more than 100M neurons. Basically, the EEG signals are mostly the result of the interaction of the cells of the cerebral cortex, which correspond to the external layer. The activity of the inner layers is difficult to extract since they're weaker due to the inverse square law and the inter-interference.

In order to extract the EEG signals, a deployment of electrodes is needed. The distribution for a typical EEG recording can be visualized at the figure 10. This configuration is called the International 10-20 reference system which is a standard while making measurements.

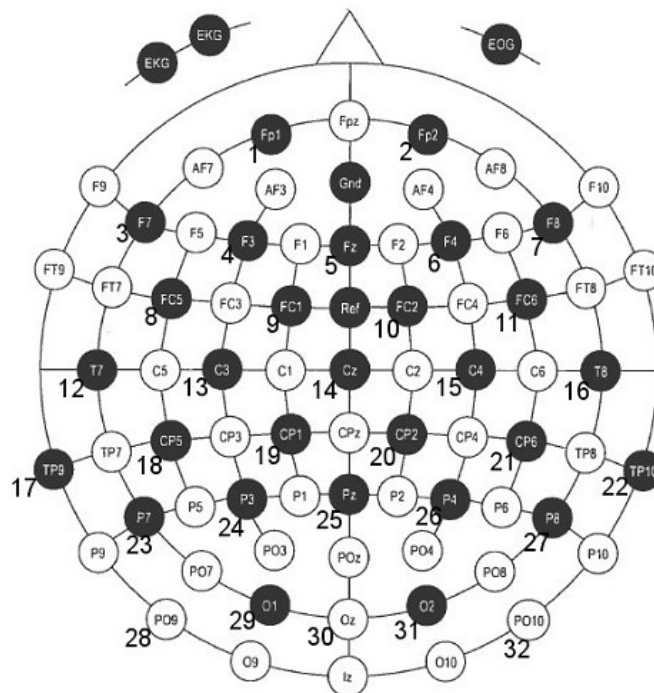


Figure 10. International 10-20 reference system for EEGs [9].

This configuration guarantees a good spatial resolution, since the signal can be strongly localized. In some particular cases it's possible to use just some electrodes considering that some signals can be more strongly present in some areas, like in the case of the alpha waves, generated at the occipital lobe. This deployment is categorized as a non-invasive method.

As mentioned, different regions create different potentials that can be mapped in order to identify patterns. These patterns can be studied seeking for abnormal parameters that can indicate the presence of pathologies. EEG are used to diagnose epilepsy, sleep disorders and another brain related diseases. Premature seizure detection has been an important topic of research for the last years, in which by identifying some conditions prior to a seizure attack, is possible to give an alert in order to take some actions with even 30 minutes of anticipation [11].

Also, the EEG signals are characterized according the frequency bands (also called rhythms) in which they appear. The following list give a detailed information regarding this:

- **The Delta waves:** Corresponds to a low frequency and high amplitude signal associated to sleep states.
- **The Theta waves:** correspond also to a low frequency signal that is presumed to provide information of sleep and daydreaming.
- **The Alpha waves:** is the prominent signal on an adult who is relaxed with eyes closed. In general, the amplitude of the alpha waves decreases when the subject opens the eyes and is alert for an external stimulus.
- **The Beta waves:** They're present when the subject is alert and attentive towards an external stimuli or under some form of mental effort, and, contrarily, it's also associated with REM (Rapid Eye Movement) sleep. At the same time, it has been related to memory processes.

Wave(Rhythm)	Freq(Hz)	Amp( $\mu$ V)
<i>Alpha</i>	7.5 – 12.5	20-200
<i>Beta</i>	13-30	5-10
<i>Delta</i>	1-5	20-200
<i>Theta</i>	4-8	10

*Table 1. Brain Waves (or rhythms).*

## 2.2 The Alpha Waves.

The alpha waves are originated by the activity on the thalamus while there exist a synchronous and coherent electrical depolarization. They're the strongest signals in between the brain waves/rhythms. They can be found mostly on the occipital lobe and it can shift anteriorly during drowsiness. It appears by three years old age at a frequency of 8 Hz and remains stable between 8 to 12 during normal aging into the later years of life. Alpha variants may include forms of one half or two time the frequency with a notched appearance [12]. Also, the mu rhythm, with a smaller amplitude, can be found around this frequency band (8 to 10 Hz), and is related to voluntary movement. It can be located at the central cortex and, since that, it does not interfere with the alpha waves directly.

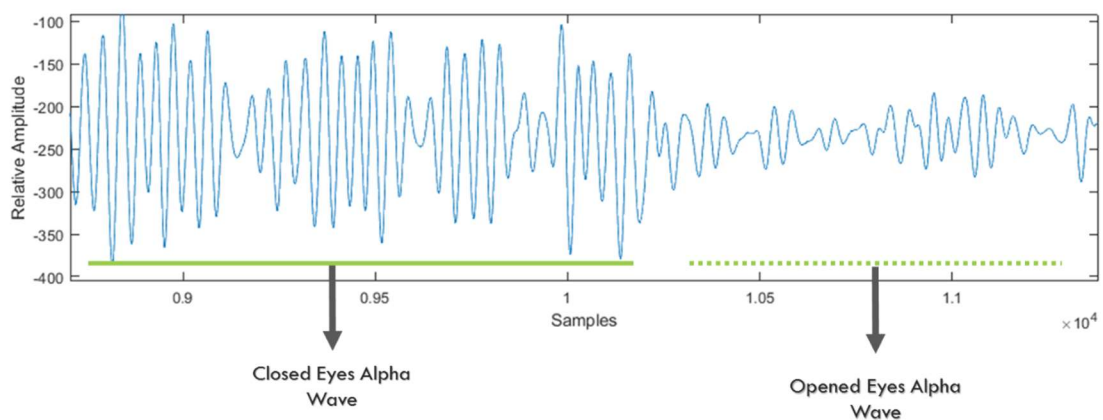


*Figure 11. Alpha waves after filtering.*

## 2.3 Extraction of the signals.

The extraction and quantification of the alpha waves can be performed using different techniques. In fact, there exist an emerging method called qEEG, that can be used to quantify the brain activity using wavelet and Fourier Transforms [12]. This approach requires a computer, which doesn't comply with the objectives of the project. Instead, a simplified and embedded solution is needed.

Indeed, the first inconvenient following previous techniques reside in the number of electrodes needed. Since the Alpha waves are mainly present at the occipital lobe, a convenient

configuration is found by locating an electrode just in the zone (Oz) of the International 10-20 system.

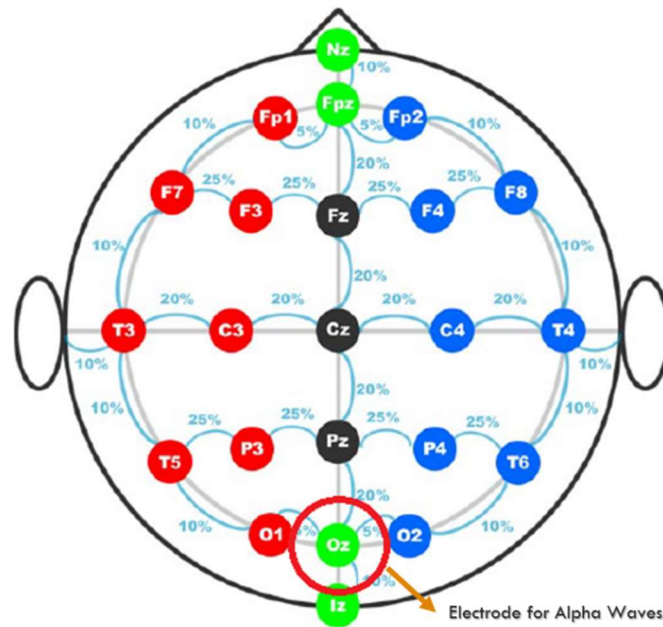


Figure 12. Alpha waves electrode location [13].

Regarding the electrodes, normally is possible to find two types:

- **Passive:** electrodes with no inbuilt circuitry.
- **Active:** electrodes with a circuitry that perform a stabilization of the signal and amplification.

For this project, the **passive** electrodes were selected given its availability and, despite the fact that they can be more affected by noise since the impedance of the configuration can be high, for the performed experiments the results were on the range of the acceptable outcomes.

Also, the passive electrodes can be classified according the materials that are made of:

- **Saline electrodes:** the main component is a sponge that is impregnated with a saline solution which creates the electrical contact with the skin.
- **Paste/Gel electrodes:** These electrodes create the electrical contact by means of a gel that transfer the signals.



The electrodes used for this project selected were **Paste/Gel electrodes**, showing good performance while collecting raw data for the first analysis and for that reason they were used through the whole project. They're made of a gel and a sticky border to guarantee the adherence with the skin.



*Figure 13. Covidien Electrodes used on this work [14].*

After the electrodes, the selection of an Analog Front End is needed. In this field of biomedical applications, they're a variety present on the market. Normally they're configurable so it's possible to use them for EMG, ECG or EEG signals. A good example of one of these devices is the ADS1398, a Texas Instruments chip, capable to read bio-potentials with 24-bit resolution on its 8 channels. In the following chapters this and some other details regarding the Signal Processing block will be explained in more details.



## 2.5 Inconveniences when working with EEG signals.

The brain signals result to be difficult to target since they may be subject easily to external interference due its small amplitude ( $\mu\text{V}$ ) and also due the internal interference that may exist in between the concurrent signals. It's possible to group them under the definition of artifacts, that are undesirable changes on the signal caused by other process in the brain or coming from a more external source. In other words, they consist in any kind of interference caused by a process different that the studied one. In the following pages, all these topics will be explained as the same as the techniques used in order to eliminate or minimize their effect on the measurements.

### 2.5.1 External interference.

**2.5.1.1 Power Line Interference (PLI):** One of the main external interferences is coming from the power source line. The lines are all around the building and they generally affect the measurements of the AFEs. Depending on the country they can be on the 50 or 60 Hz band. These signals can block a clear reading of the EEG, and for that, they have to be considered at the setting up moment.

The most recurrent approach for this purpose is the use of Notch Filters (Band-Stop Filters). Also, some other techniques can be used, like Time Domain Subtraction, Regression Subtraction and Sinusoidal Modeling. In this work, this interference has been cleared by using notch filters, since it's easy to implement and doesn't require high computational cost.

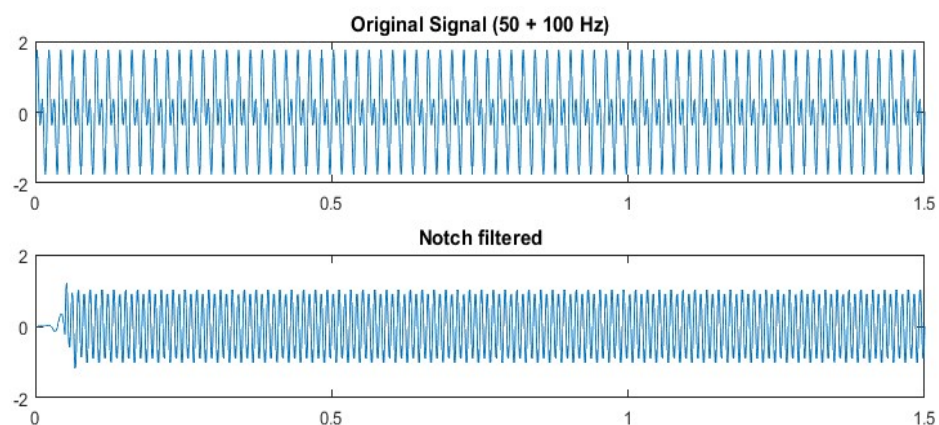


*Figure 14. Notch Filtered signal.*

## 2.5.2 Internal Interference.

**2.5.2.1 Eye Blink Artifact:** An eye blink artifact is generated by the electrical potential produced by the vertical movement of the eye [12]. Normally, the eye functions as an electrical dipole with relative positive of the cornea compared with the retina. The potential created is a DC potential of higher amplitude (mV) than the amplitude produced by the brain( $\mu\text{V}$ ).

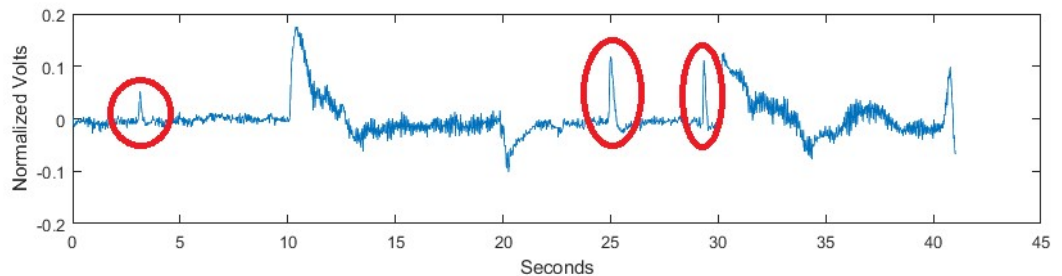


*Figure 15. Eye blink artifacts on EEG.*

This artifact results to be difficult to eliminate since the amplitude is high and it can appear in the frequencies on interest. Nevertheless, two techniques were meant in order to minimize the effects on readings and interpretation, especially when the targeted signal is the alpha waves:

- **Gap-Band detection:** Consist in a technique that identifies the presence of the blink by taking in consideration the Power Spectral Density (PSD) of the different frequencies. If the PSD shows the presence of energy on the band between 2-12 Hz, it's possible to assume the signal constitutes a blink. In the other side, if the signal just shows energy at the alpha waves band, it's possible to assume that only the alpha waves are present.

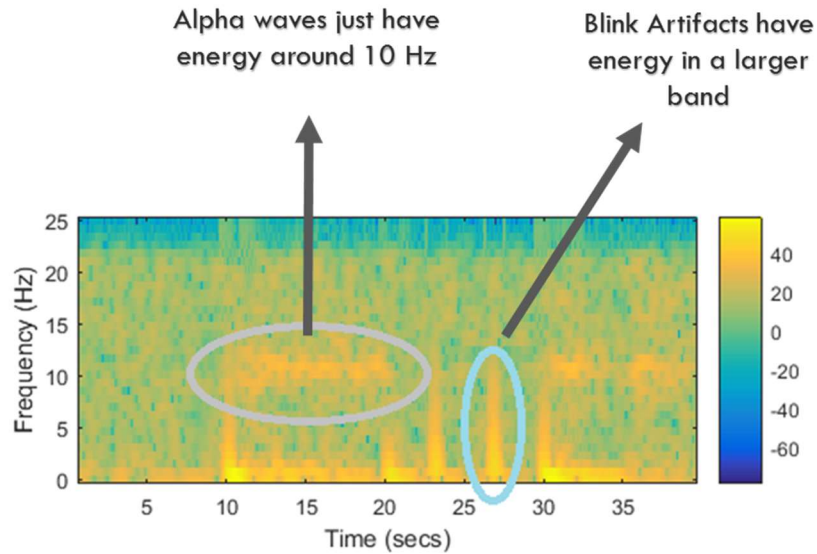


**Figure 16.** Artifacts on the spectrogram of the signal.

- **Low pass detection:** Since the blinks result to be a transitory artifact, it's possible to eliminate them, particularly when using a detector, by using a 'low pass decision filter', i.e., in order to detect the alpha waves, the signal has to be present for a considerable period of time.

**2.5.2.2 ECG artifacts:** when the aim is to capture the brain signals, sometimes it's possible to encounter the presence of the signals of the hearth muscle. To eliminate them new methods are available, like the use of a modified Independent component analysis (ICA) [15]. Fortunately, in this project this artifact was not strongly present and did not affect the readings.

**2.5.2.3 EMG artifacts:** These artifacts are the result of the muscular activity while performing EEG. They consist on a series of spikes that may affect the reading of an EEG signal. This is also difficult to remove, but latterly some techniques like the Surface Laplacian and ICA implementations [16] are being study for this purpose. Also, during the project, this artifact did not represent an important issue and any elimination method was applied.

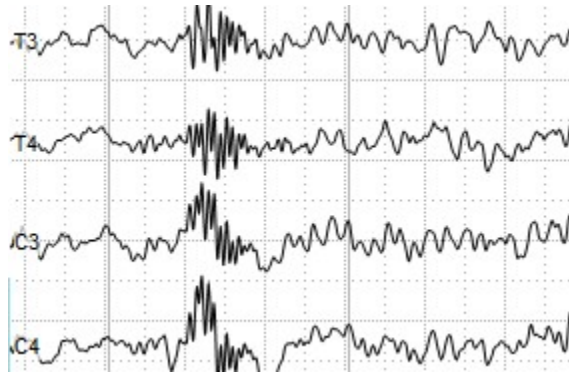


Figure 17. EMG artifacts [17].

**2.4.2.3 Ground lead off and electrode slicing:** A correct coupling with the tissue is important since it will allow the correct acquisition of the voltage values. A good coupling is characterized by a low impedance. In order to have a good connection is recommended to have an electrode-skin impedance below 10KOhms. Also, any kind of slicing (or movements) on these electrodes can generate spikes that will corrupt the desired signal. In the case of the Ground electrode, any alteration can cause a shifting on the mean value of the signal, generating distortions on the time domain of the signal, which is at the same time an inconvenient while making a visual interpretation of the signal. In the case of the measurement electrodes, any kind of slicing or temporal detachment of the electrode will cause the contamination of the environmental signals. Mostly, this signal corresponds to the 50/60 Hz PLI.

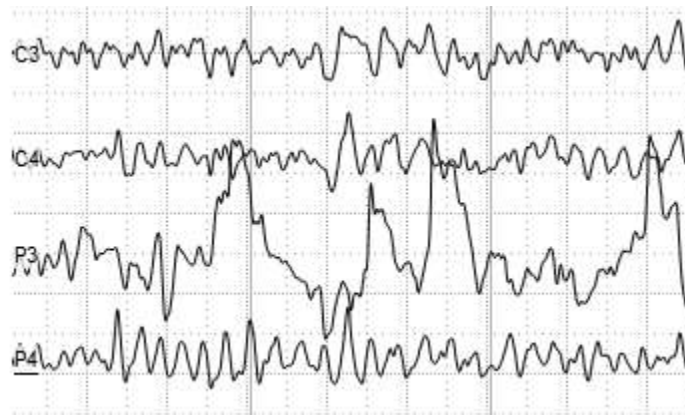
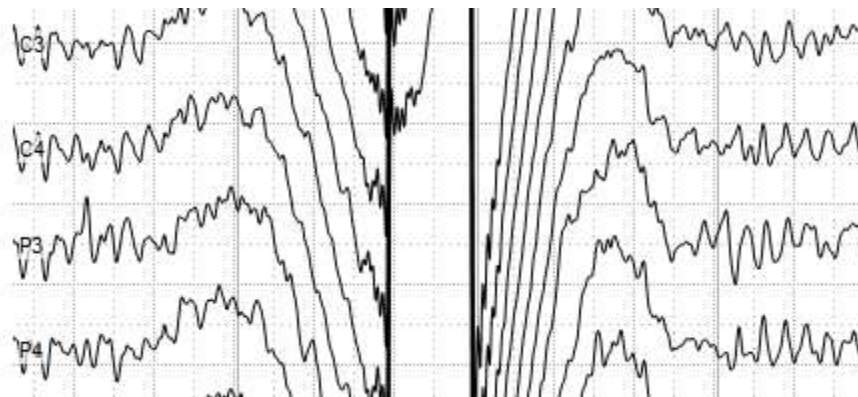


Figure 18. Electrode slicing artifact [17].



**Figure 19.** Ground Lead off artifact [17].

### 3 EEG Board, design and features for the project.

Given the requirement of the current work, and considering the classical structure for reading biomedical signals, the hardware required must have the following scheme.

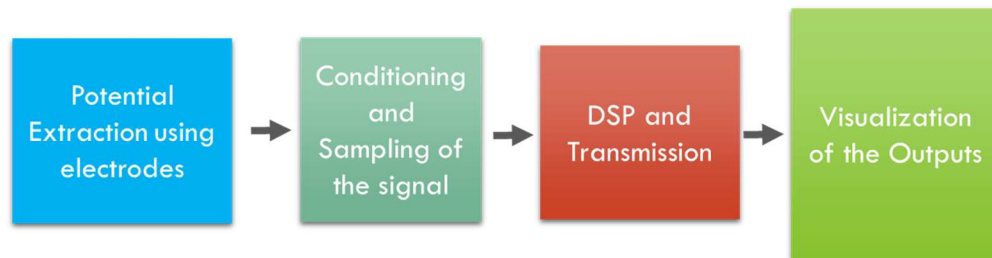


*Figure 20. Pipeline for extraction of EEG signals.*

A typical EEG scanning, using the full number of electrodes require in between 10 to 20 electrodes. Since this work was based on the detection of the alpha waves (Zone Oz), just one electrode was needed (see Chapter 2, section 3).

Regarding the sample frequency, since the targeted signal is on the range of frequencies of 7.5 and 12.5, the sampler, obeying the Nyquist criteria, the sample frequency has to be at least the double of the targeted signals. Nowadays, these values are easily accomplished by almost any ADC converter. Indeed, the sample frequencies used for EEG readings are in the range of 100 to 1kHz [18].

Summarizing the requirements, It's possible to say that the hardware must be able to sample the bio potentials in a given minimum frequency and to have a powerful microcontroller in order to perform the DSP on the inputs as the same as being capable of streaming the information to an output device.

Thanks to a previous work, it was possible to have access a board, that was complying with the previous requirements. This board has been designed for the acquisition of bio potential on the MICREL LAB of the University of Bologna, from here ahead called the EEG board.

### 3.1 EEG board Hardware Scheme.

The main components correspond to the ADS1298, the Analog Front End and the Cortex M4 based STM32F407 microcontroller. Some other components are also available for other type of measurements that will be explained below:

3.1.1 **The ADS1298:** is a multichannel (8 Channels) simultaneous sampling 24 bit, delta sigma ADC with build in Programmable Gain Amplifiers (PGAs), internal reference and onboard oscillator. It was especially designed for EMG and EEG signal acquisition. This device can perform sampling up to 32KSPS and can deliver the sampled information through a SPI interface.

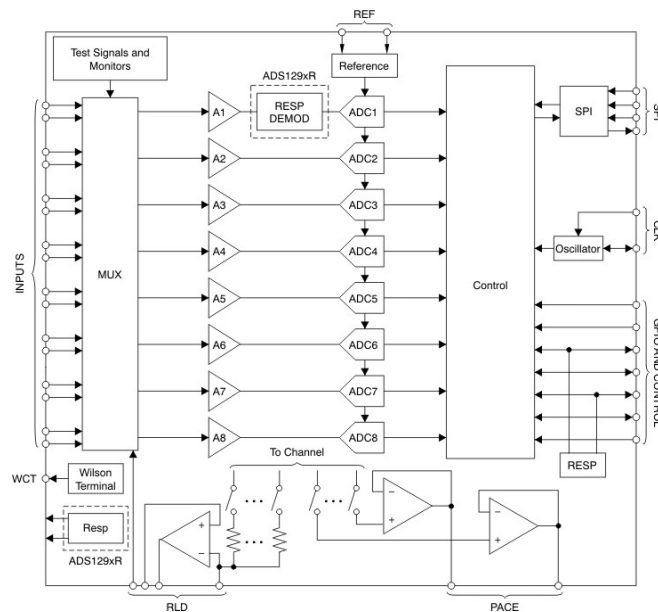


Figure 21. The ADS1298[19].

3.1.2 **STM32F407VGT6 microcontroller:** This device, widely used in the industry due to its advantages, is a 32-bit M4 Cortex CPU-based microcontroller, with FPU, working frequency of 168 MHz, memory protection unit and DSP instructions. It has up to 1 Mbyte of Flash memory and up to 192+4 Kbytes of SRAM. The most important features can be summarized in the following list:

- Ultra High Data Transfer, with a 7 multi-AHB (Advanced High-Performance Bus) level bus matrix and DMA controller (Direct Memory Access).
- The FPU supports all the single precision operations and is capable to do the format conversion for floating point and fixed point.
- High flexibility to reduce the energy consumption. Contains a backup 4Kbyte SRAM memory for standby mode. It has also an RTC (Real Time Clock) with a power consumption below 1  $\mu$ A.
- It has several peripherals, from which the most important ones are: USB OTG, Ethernet 10/100, 6 UART ports, 3 SPI ports, 3 I2C ports, 2 CAN, 2 12bit DAC, 3 12bit ADC with 2.4 to 7.2 MSPS, 17 timers and 5 GPIOs ports.

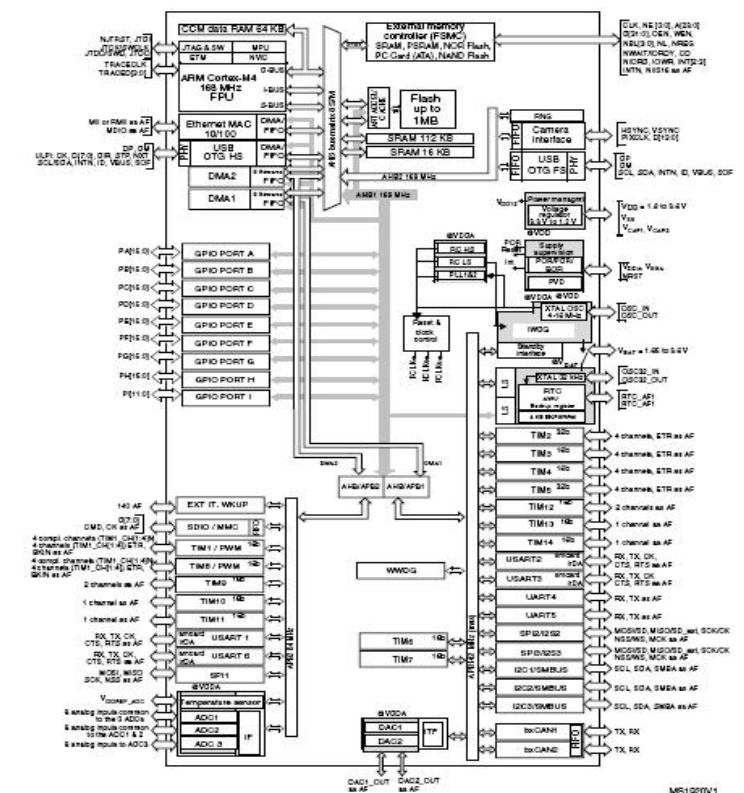
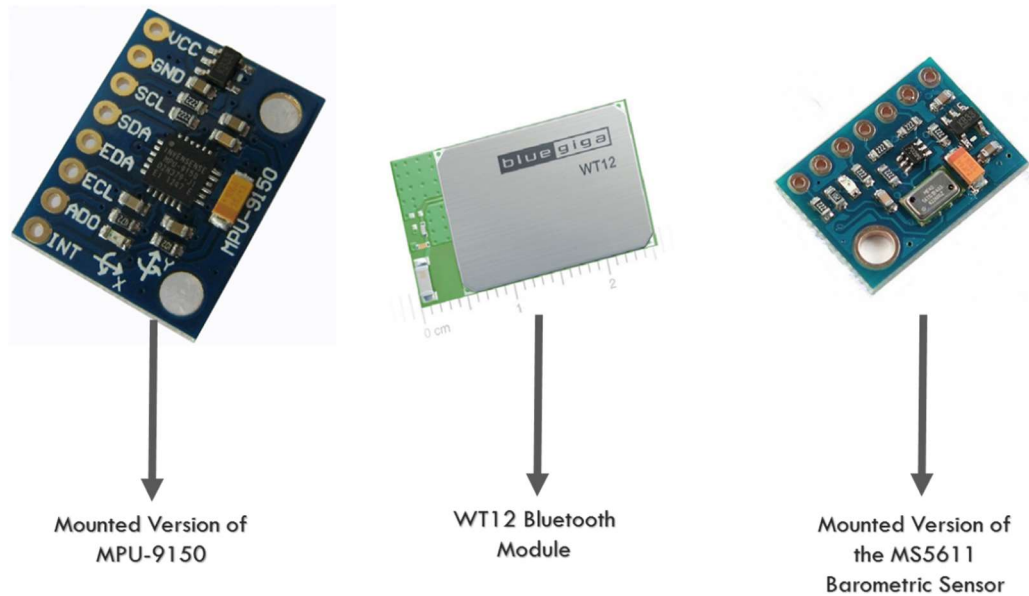


Figure 22. STM32F407 Block diagram [20].



3.1.3 **Pressure and accelerometer sensors:** The board has an MS5611-01BA barometric pressure sensor with a high resolution module (10 cm), fast conversion (1ms) and low power consumption (1uA) with I2C and SPI communication ports. The accelerometer is a MPU-9150 9-axis motionTracking device, which combines 3-axis MEMS gyroscope, 3-axis MEMS accelerometer and 3-axis MEMS magnetometer with a Digital Motion Processor(DMP™). Is widely used in smartphones and tablets. Is capable to perform 16-bit ADC and has a I2C communication port.

3.1.4 **Bluetooth Transcriber:** The Bluetooth devices used is a BlueGiga WT12, a BT 2.1 with EDR (Enhanced Data Rate). The maximum data rate is 3Mbps. It has a transmit power of +3dBm and approximately 30 meters or range in line of sight thanks to its integrated antenna.



*Figure 23. Other modules of the EEG board.*

### 3.2 Working Principle.

The process of acquisition of the signals can be summarized in the following scheme:

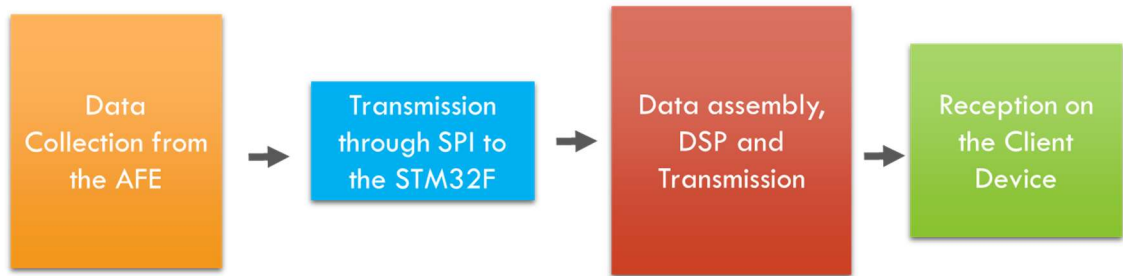


**Figure 24.** Working principle of the board.

The input signal enters to the Analog front end (ADS1398) through a cable connected to the HDMI connector. The AFE perform the reading in a period according the programmed sample frequency. Once the data is ready it's send through the SPI bus to the STM32 microcontroller in a Two-Complement format.

The microcontroller receives the data, ensembles the bits and recover the value for each channel. Once this is done, the DSP can be performed. In this project the typical DSP tasks are Filtering, Envelope extraction and FFT.

After this process, the information is ready to be streamed to the client. This is done using the UART port of the microcontroller.

The UART port is connected to the Bluetooth which streams the data. In this work we used as a client an Android based Tablet to store the data and also to visualize the EEG signals on real time.

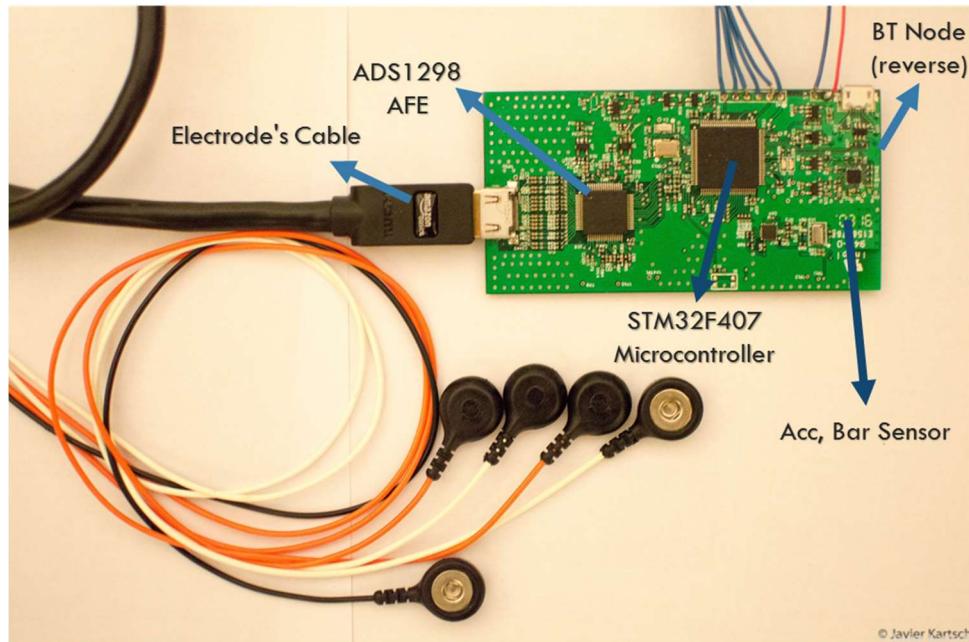


*Figure 25. EEG Board PCB.*

This device can be adjusted in order to meet the requirements of the diverse measurements. In this project the EEG signals were of interest but the board can also perform measurements on mostly all the bio potentials mentioned in the chapter 2.

### **3.3 Firmware architecture.**

The implemented firmware follows the working principle on the previous section. In the figure 26 is possible to see in details the implementation of a State Machine (SM) to properly manage all the tasks.

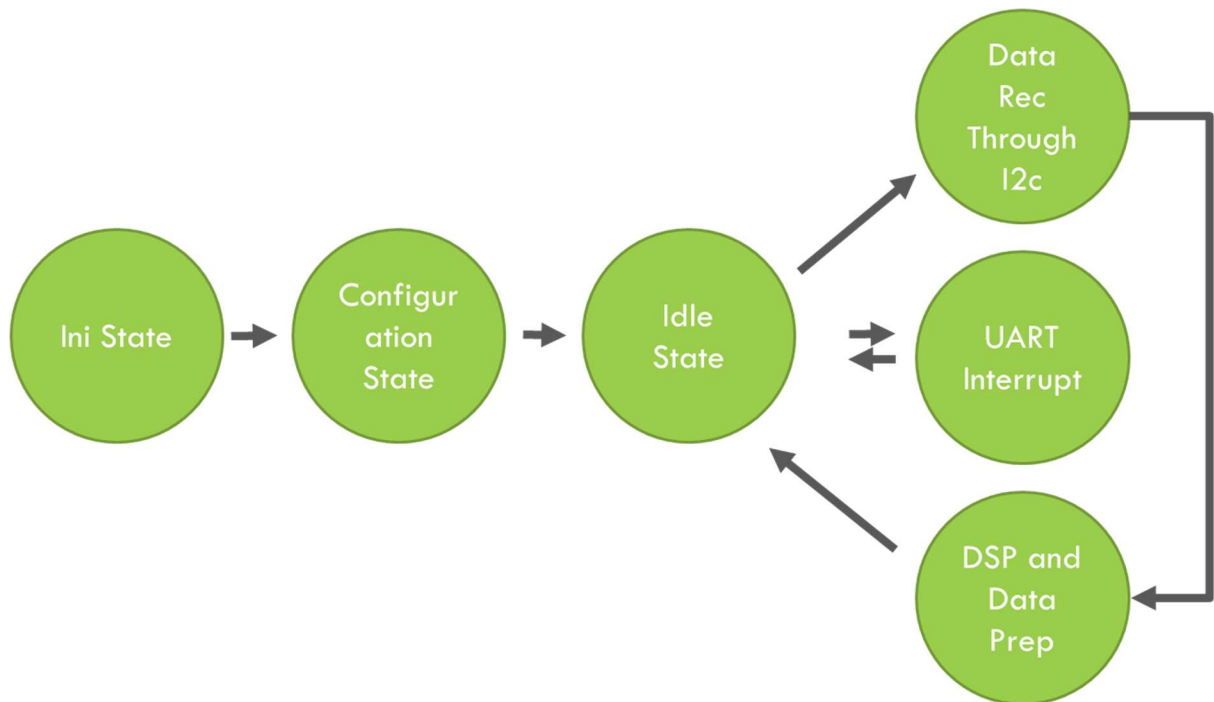


**Figure 26.** State Machine on the microcontroller

After the power up, the initialization of the variables is done before to enter to the state machine. The states guarantee the realization of the different task needed in order to retrieve the sampled frequencies at the AFE.

- **Init State:** this state will create some local variables that are needed through the process.
- **Configuration State:** Here, all the commands for the configuration of the ADS1298 will be send through the SPI bus of the microcontroller. The AFE works in a continuous mode, which implies that as soon the ADS1298 have a reading it will transmit to the SMT32 microcontroller. There are some other modes, so this parameter has to be set as the same as the sampling frequency, PGA values and the reading source (which can be auto generated square test signal or the signal form the channels properly).
- **Idle State:** the SM will keep the microcontroller in idle until some event triggers a jump to the other states.
- **Data Reception Through SPI:** the device receives data from the AFE when a reading is available.

- **DSP and Data preparation (packet):** Once the data is received from the AFE and assembled it will be sent through the UART port of the STM32 using an interruption, which in turn will arrive to the Bluetooth module to finally be sent to the client. In the final implementation, the DSP routines were added in order to perform the detection of the Alpha Waves.

## **4 Android application.**

After the extraction of the values from the sampled signals are required an end device to record the information and visualize the parameters on real time. There are many available options for this purpose. A desktop computer can perform all the tasks for the reception and visualization required, but its lack of portability made it not suitable for this project. Instead, helped by the big improvements on the mobile technology, nowadays is possible to find devices that can be used for this purpose. Smartphones and tablet have a high computational power with multicores and large memory for storing the retrieved data as the same as good connectivity using the Bluetooth connections as peripherals.

The choice afterward will be the selection of the device with a given Operating System (OS). On this matter, given the availability of android devices, and the extended libraries existing on the internet, it was concluded that platform would be an excellent choice for the development of the desired application.

In the following lines, all the aspects related with the android application used in this project are going to be addressed.

### **4.1 Main parts and working principle.**

The development of the applications obeyed two main requirements. The first, the capability to receive and visualize the signal, and the second, the ability of storing the information for a latter analysis. In the following figure is possible to see the developed application following these requirements. The visualization screen is based on the MPAndroidChart [21].

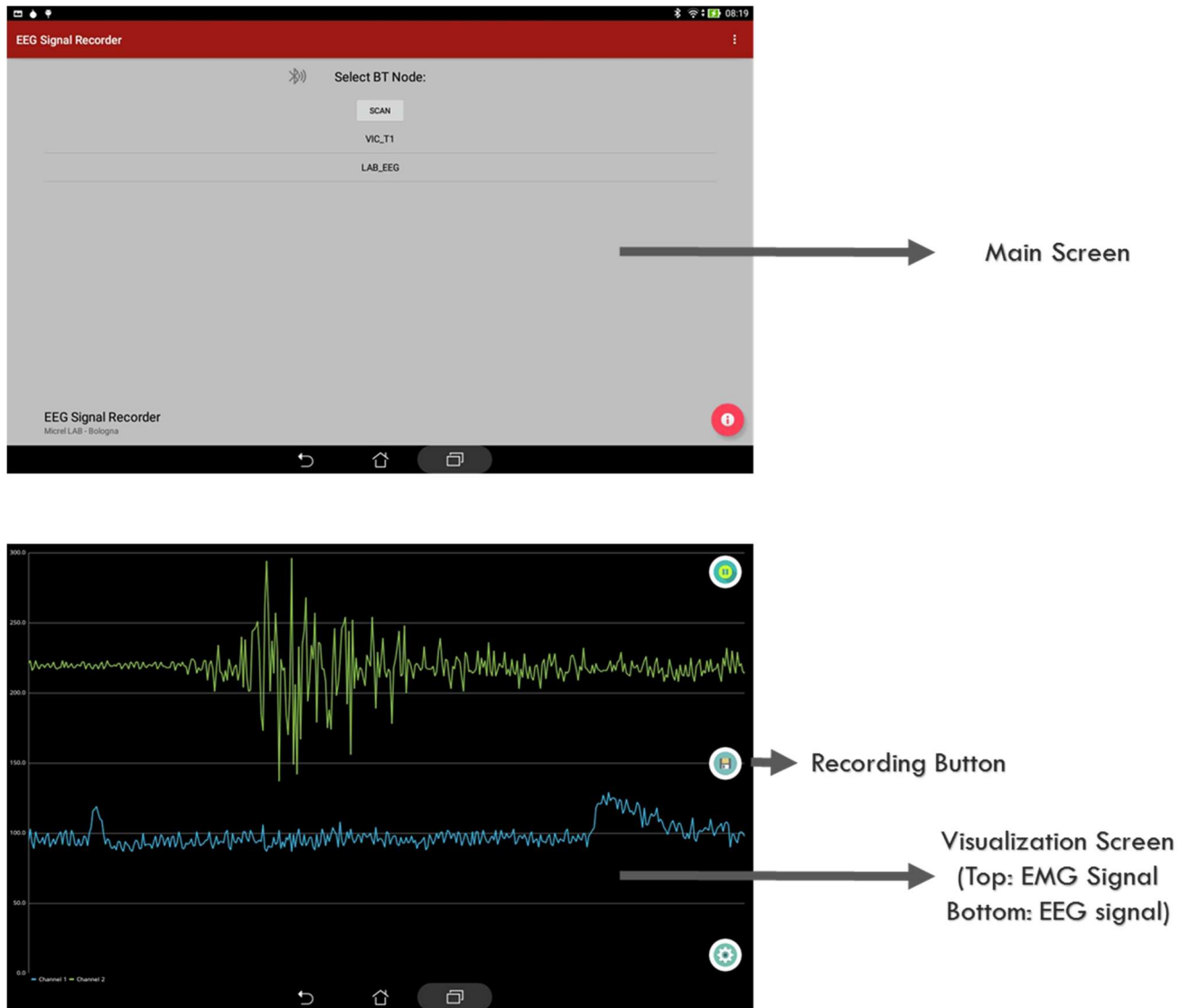


**Figure 27.** Android EEG Reader.

However, there are some hidden features that were needed and the following list summarizes all of them:

- Create a Bluetooth Client for connecting with the EEG Board.
- Receive the streamed data from the EEG Board with a data rate of 500 Readings/Second.
- Visualize the 8 channels received in a form of waves of the screen.
- Adjust the visualization parameters (offset, magnification, down-sampling rate, X and Y limits of the visualization on the screen).

- Scroll the plotted signal giving space for the new values.
- Storage of the received reads in a file for a latter analysis.
- The application can work with any device that has an Android version > 4.2.

The main and extra features were needed in order to have a more intuitive understanding of the received signals.

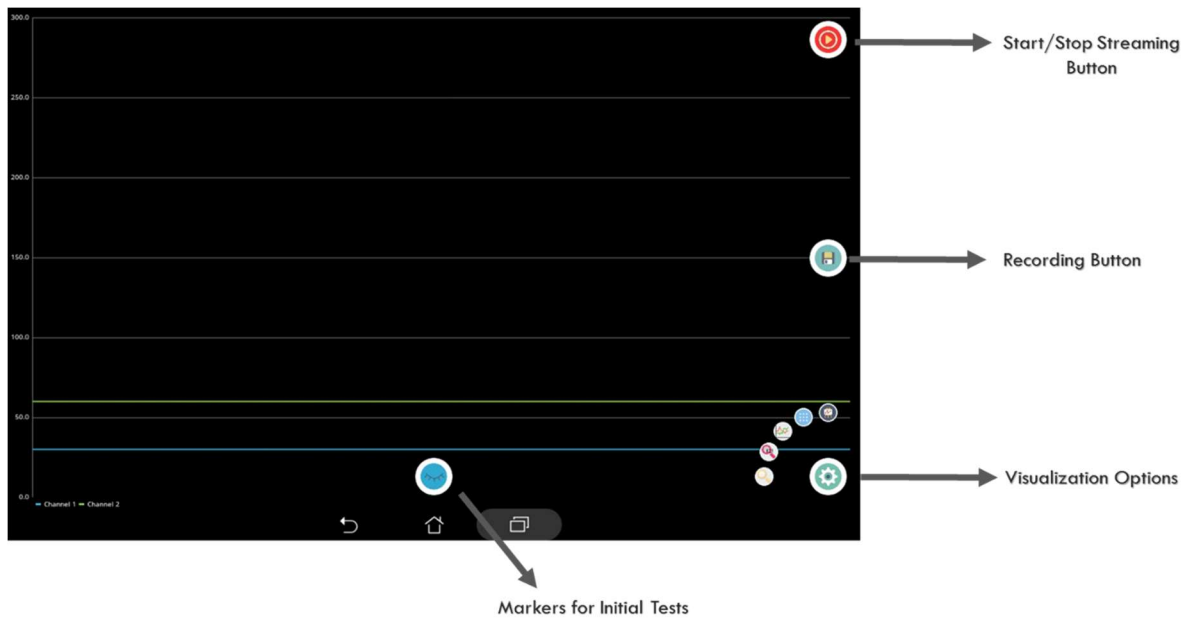


Figure 28. Visualization Screen and options on Android EEG Reader

## 4.2 Steps for the reception of the values form the microcontroller.

**4.2.1 Bluetooth Connection:** Initially, it's important to try separately the BT connection, that is working behind the application. The Android system for managing the Serial port can be summarized in the followings scheme:

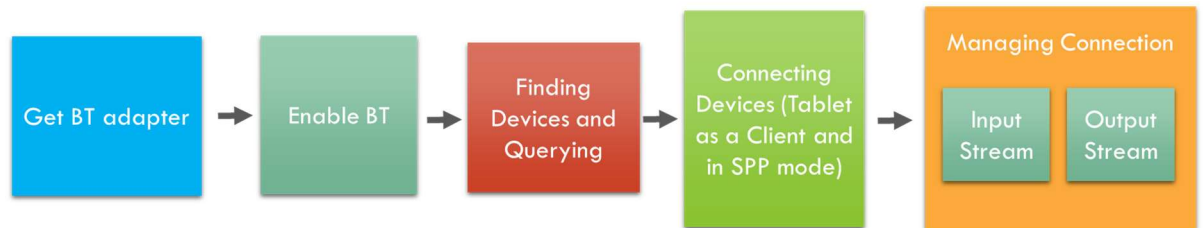


Figure 29. Bluetooth connection pipeline.



First, the application checks the availability of a BT adapter. Once its presence is guaranteed by the system, the application will enable it to find the active devices surrounding the area of coverage. After this, once selected the device to connect, the system will initialize a client mode connection with the EEG board using a Serial Port Profile mode (SPP). The SPP will emulate a typical wired serial communication.

**4.2.2 Application Tasks:** after the BT connection is established, the user can select the number of channels to be shown. The reception of the data is executed in a different thread than the other tasks to assure a real time response. The use of different thread will allow a parallelization of the tasks through the different cores available on the device. The main thread is responsible for the plotting the values of the received files, store the information and change the visualization parameters and the second thread is in control of the reception of the readings. Essentially, the characters are received one by one until the number of expected values has been reached. The following routines are in charge of assembling the short type received values into signed integers.

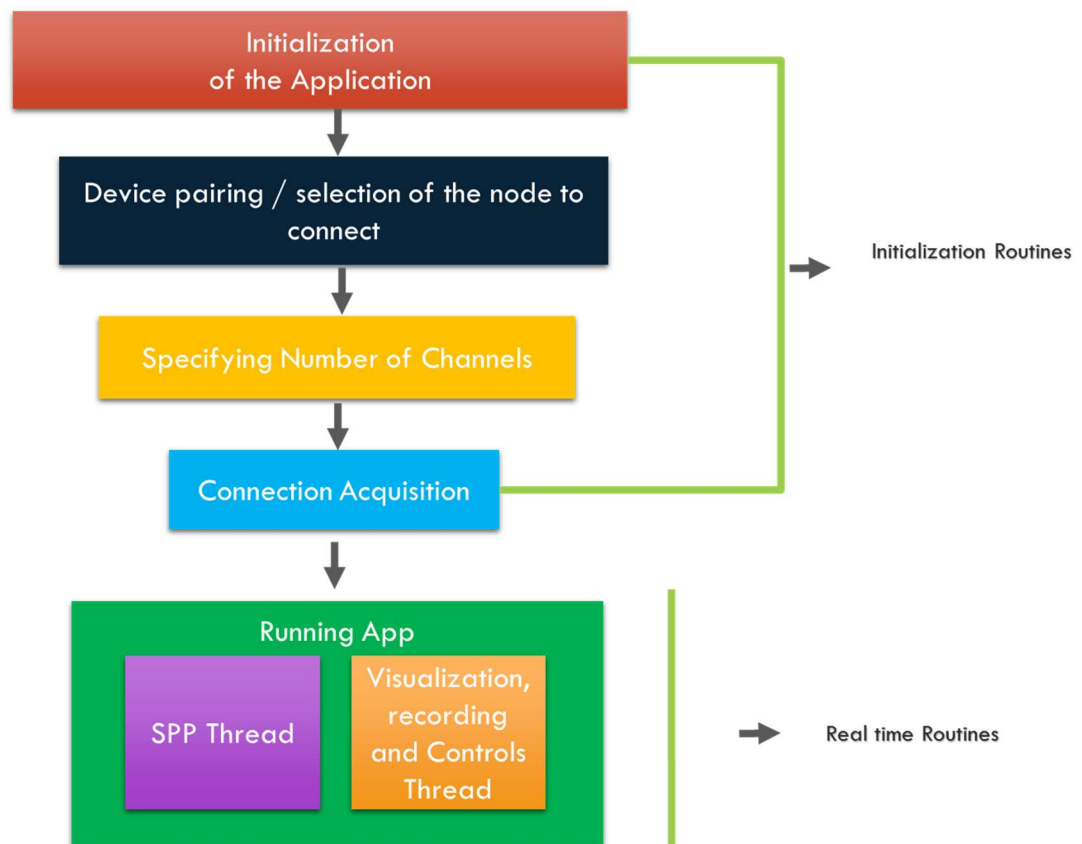


Figure 30. Application flow diagram.



Figure 31. Implemented application.

### 4.3 Modification for evaluation of the final performance.

For evaluating the performance of the final implementation, i.e., the final firmware on the EEG Board, some modifications have been done. The connection and reception algorithms remained the same but It has been added some new features that will allow an automatized test.

The test is performed by using some sonorous alert indicating the user that is time to open/close the eyes. The periods of test have a length of 15 seconds for each action.

Right after the start, the program will count the number of received values. According to the output values a counter will accumulate the predicted feature. All the values will be summed after all periods.

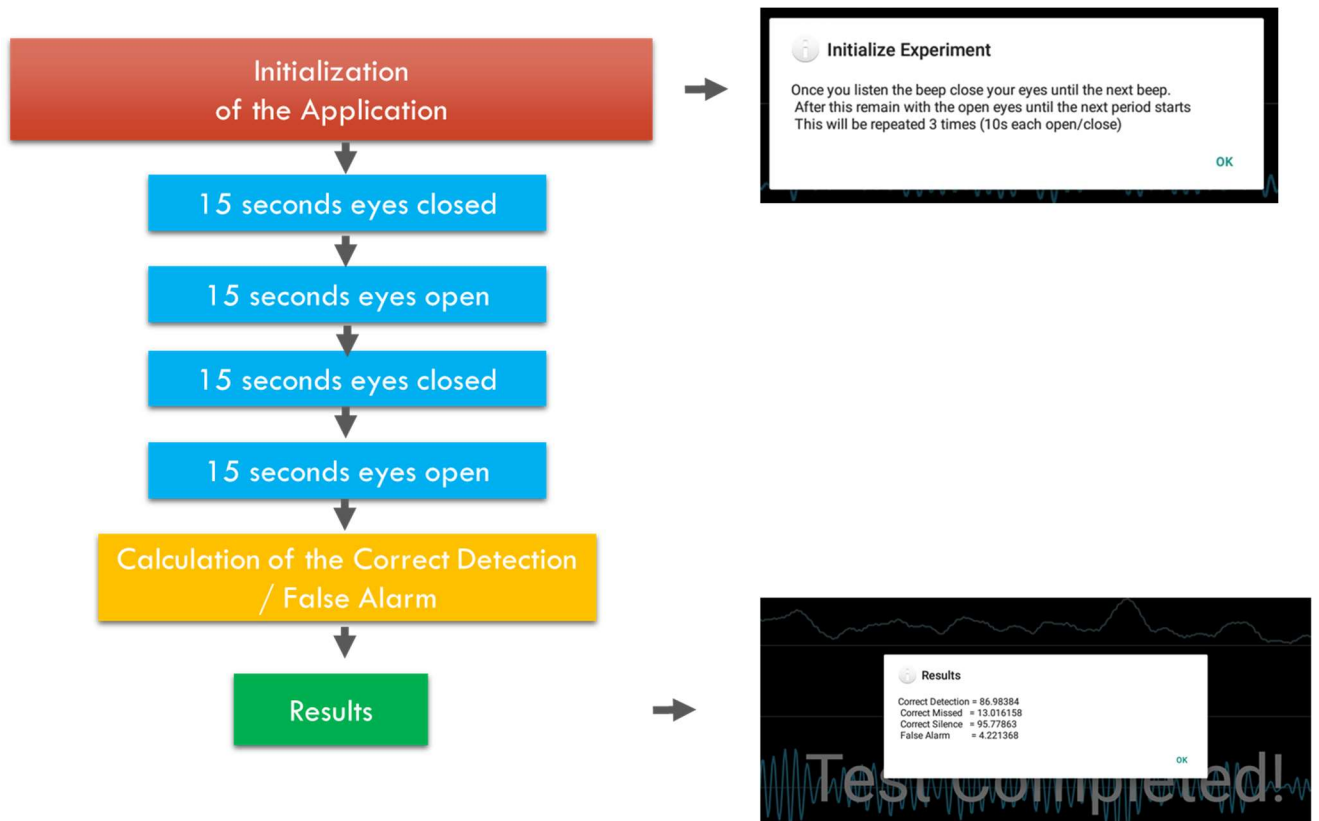


Figure 32. Test mode of the EEG Signal manager.

## **5 Data Collection and modeling on Matlab.**

In order to minimize the number of approaches for a final implementation, some exploratory approach has to be introduced. Using the current tools for data analysis is possible to obtain results in an offline mode which may suggest the best method to be translated into the microcontroller.

With this purpose, taking in consideration all the tools available on MATLAB, it was decided that a good method to understand and classify the best ways, study the drawbacks and the impact of the different approaches will be by creating some models with this software.

In the following pages, all the implementations studied will be exposed as the same as the results. The tested methods can be classified in two general groups, threshold based approaches and decision tree based.

Before introducing the implementations, it will be presented the methodology for taking the trials from the test subjects and the metrics used to evaluate the different models.

### **5.1 Data Collection.**

The initial data was collected using the EEG board with the basic firmware, only streaming the raw data from the electrodes. No DSP were used since the aim was to have the original data. On the other side, the android application was used for collecting the incoming data and store it in a file (without the test module).

The subjects were using the minimum number of electrodes, as it was originally stated, locating the reading electrode on the zone Oz, a differential electrode placed on the forehead as the same as one electrode for reference placed on the earlobe.

The subjects were located on a peaceful environment with no distractions and in absence of apparent external electric interference. The trials consisted on two cycles of open/close events, each one of 10 seconds, with a maximum time length of 40 seconds. As a matter of example, the following figures will help understanding this process in which is possible to see the readings plotted and scaled in order to have the x-axis in seconds.

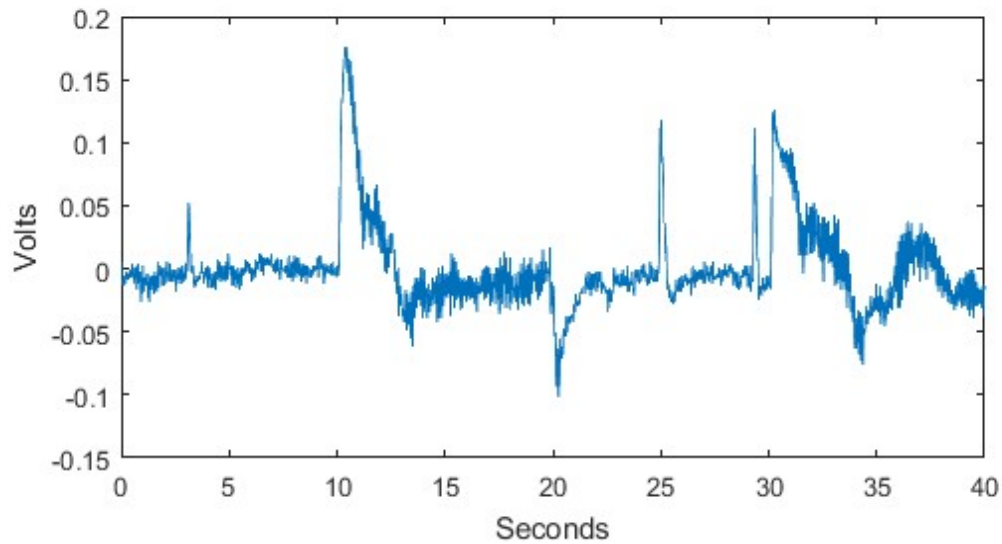


**Figure 33.** EEG signal extracted using the EEG Board.

A better understanding of the energy components came from the use of spectrograms. They show the energy of the signal for different frequencies on time. The colors that tend to the red have more energy than the other ones.

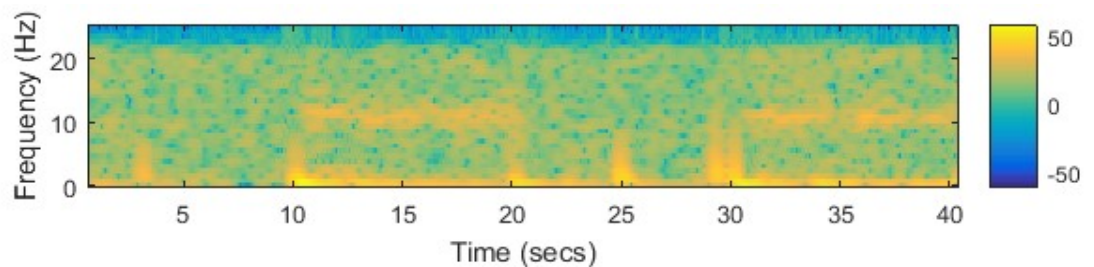


**Figure 34.** Spectrogram of the extracted data.

Here, it's possible to see the presence of two important components, the first, the presence of the Alpha waves with a frequency around 10 Hz, in the time from  $t=10$  to  $t=20$  as the same as  $t=30$  to  $t=40$ , the second component corresponds to the spikes at  $t=2.5$ ,  $t=25$  and  $t=28$ , which correspond to blink-eye artifacts.

The trials were performed four times for each test subject. For the data collection, three test subjects had participated. They were all on the range of age of 25-35 years old and did not have any apparent medical condition that may affect the experiments.

## 5.2 Establishing metrics for determining the performance.

Since the approaches that were intended were mostly based on binary decision, the following metrics were used:

- **Sensitivity and Specificity:** This metric is used for the statistical measurement of the performance on binary classification. The sensitivity corresponds to the part of the measurements that are correctly classified, i.e., eyes closed on this work. It can be calculated using the following equation.

$$Sens = \frac{\textit{number of true positives}}{\textit{number of true positives} + \textit{number of false negatives}}$$

The specificity corresponds to the part of the measurements that are correctly classified as negatives, i.e., eyes open on this work. The value can be obtained by:

$$Spec = \frac{\textit{number of true negatives}}{\textit{number of true negatives} + \textit{number of false positives}}$$

- **Score over Sensitivity and false alarm:** This value was the result of the subtraction between the sensitivity and false alarm (1-specificity) with the aim to see the balanced metric regarding a binary class prediction.

$$Score = Sensitivity - false\ alarm$$

In a less extensive manner, some *M*-ary classification was also done. The metric used in this case is explained as follows:

- **Confusion Matrix:** it was also studied other implementations different from the binary ones. For that reason, the confusion matrix results to be more suitable since it can show data for more than two classes. The confusion matrix consists in a table organized in rows and columns. The rows represent the instances in an actual class and the columns represent the instances in the predicted class.

		Predicted Class		
		Cat	Dog	Rabbit
Actual class	Cat	5	3	0
	Dog	2	3	1
	Rabbit	0	2	11

Figure 35. Confusion matrix example.

### 5.3 Threshold Based approaches.

The threshold approaches are result from the comparison between some present value (or extracted) and a fixed value (the threshold). In order to accomplish that, non-oscillatory features of the signal were used. Two main methods were tested:

- 5.3.1 Threshold using PSD:** This method relies on the evaluation of the energy of the signal by using the **Power Spectral Density**. To extract the PSD, first, the Fast Fourier Transform is calculated for a sequence of numbers with a given sample rate.

$$X_k = \sum_{n=0}^{N-1} X_n e^{-i2\pi kn/N}$$

**Where:**

$k = 0, \dots, N - 1$  are the Transformation bins index,

$X_k$  = complex output of the transformation (bins),

$X_n$  = Input values.

The PSD (estimation) will be obtained by taking the square magnitude of the complex outputs of the FFT.

$$PSD = |X_k|^2$$

For practical purposes, the **Short Time Fourier Transforms (STFT)** is used in offline data, which is a calculation of the FFT on short time periods of the signal using an overlapped window. This process leads values of energy for small frequency regions that gives more intuitive results. As before, in order to obtain the PSD values, a square magnitude is applied. In the case of online data, the first implementation is utilized.

$$STFT \{x[n]\}(m, \omega) = \sum_{n=-\infty}^{\infty} x[n]w[n - m]e^{-j\omega n}$$

**Where:**

$x[n]$  = input signal,

$w[n]$  = window function.

The STFT algorithm used on this project was developed by of Hristo Zhivomirov and shared through the file exchange program of MatWorks. It requires as input the values of the signal (x), sample frequency (fs), window length (wlen), hop size (h) and number of FFT points (nfft) [22].

$$STFT_{lib}(x, wlen, h, nfft, fs)$$

The output of this algorithm will give a vector containing values of energy for the different frequencies. The algorithm reported at figure 36 will focus just on the interval of frequencies corresponding to the Alpha waves. From all the values contained in this, the maximum is selected.

Taking this into account, the algorithm after extracting the PSD follows the next scheme in the MATLAB scrip:



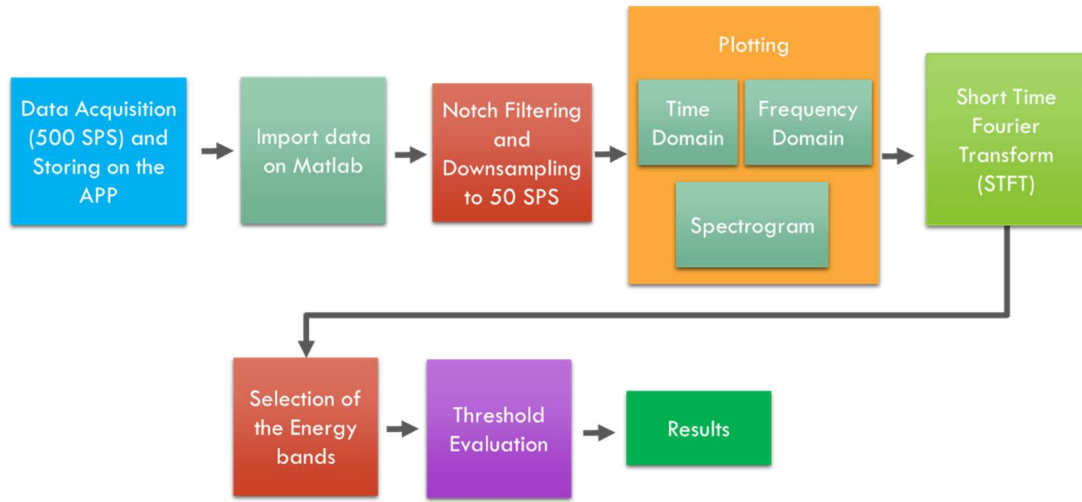


Figure 36. PSD Threshold algorithm.

The best value for the threshold was found by evaluating the sensibility and specificity with the different trials. The results are shown in the following table:

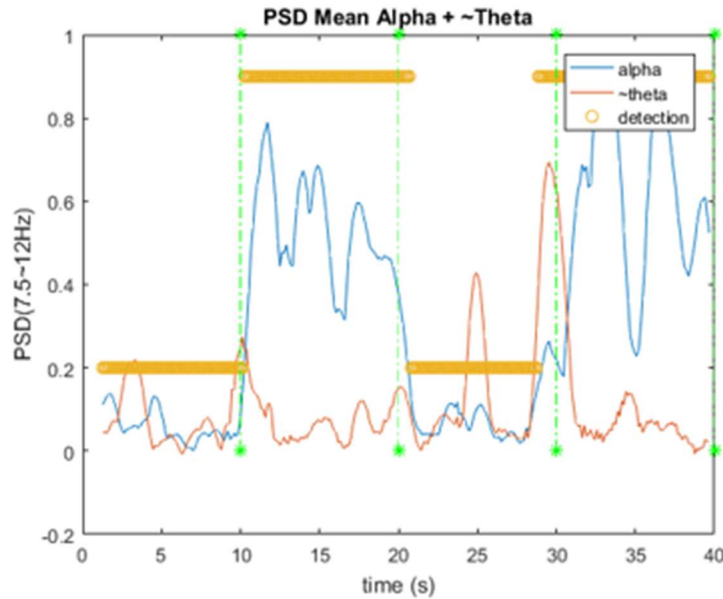
Method	Details (threshold)	Sens	Spec	Score
PSD	0.1	0.992	0.741	0.734
PSD	0.15	0.984	0.903	0.887
PSD	0.2	0.953	0.935	0.888
PSD	0.3	0.868	1.000	0.868

Table 2. PSD threshold comparison.

From these results it possible to assume that the best value for the threshold ( $th$ ), according to the Score criterion, is on **the range of 0.15 to 0.2**. The figure 37 has been created using  $th = 0.15$ . The results were achieved by applying values at table 3 on the Short Time Fourier Transform. They were fixed by using the spectrogram in order to guarantee the presence of the alpha waves.

Parameter	Value
Sample Frequency (Hz)	50 (down-sampled)
Window length	128
Hop size	6
Number of FFT Points	128

Table 3. PSD threshold comparison.



**Figure 37.** PSD threshold detector implemented in one trial.

**5.3.2 Threshold using an Envelope approach:** this is a simple approach in which the original signals is filtered to focus only on the alpha waves frequency (7.5 – 12.5) and later, the envelope of it is extracted. In this project, the RMS envelope was used. As usual, several types of filters can achieve be used for the filtering. For the purpose of this work, it has been selected a Finite Impulse Response (FIR) filter since it's recommended for Bio-potentials by other investigations [23].

The output of Finite Impulse Response filter is characterized by the following equation:

$$y[n] = \sum_{i=1}^N b_i \cdot x[n - i]$$

**Where:**

$y[n]$  = output signal,  $x[n]$  = input signal.

$b_i$  = filter coefficients.

$N$  = order of the filter.

The order of the filter (N) may be a critical part on this. Since low orders give bad performance due that sensitiveness of the small involved bandwidths, higher orders are needed. At the same time, high orders will require more computational power while dealing with real time applications. Also, the group delay may large. For these reasons, a trade of in between these parameters in needed.

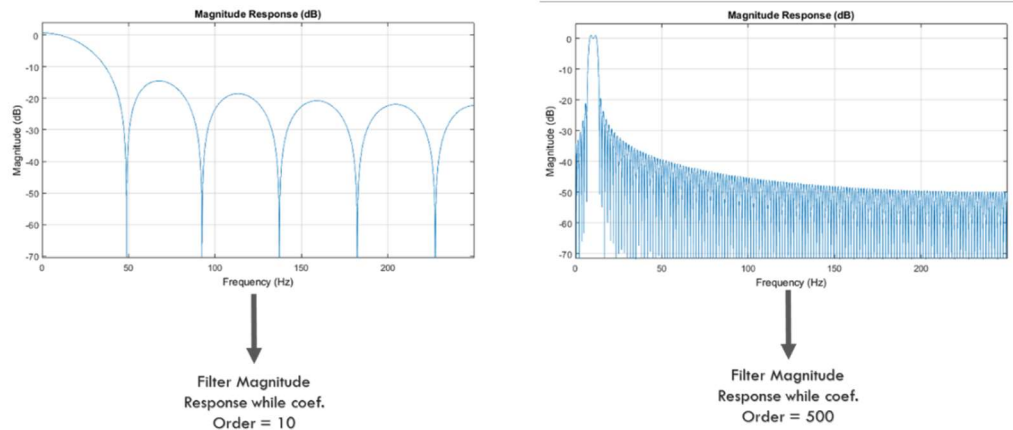


**Figure 38.** Magnitude Response of different filters.

Using MATLAB is possible to easily determine the values  $b_i$  by means of the function `fir1`. This function uses a Hamming window to design a  $n$ th-order filter.

It requires as inputs the cutoff frequencies in a normalized format. The values for filtering the alpha waves were calculated as it follows:

$$fn1 = \frac{LeftPassFrecuency \times 2}{Sample\ rate} = \frac{7.5 \times 2}{500}$$

$$fn2 = \frac{RightPassFre}{Sample\ rate} \times 2 = \frac{12.5 \times 2}{500}$$

Once obtained these values, it's possible to apply the function.

$$bi = fir1(N, [fn1 fn2])$$

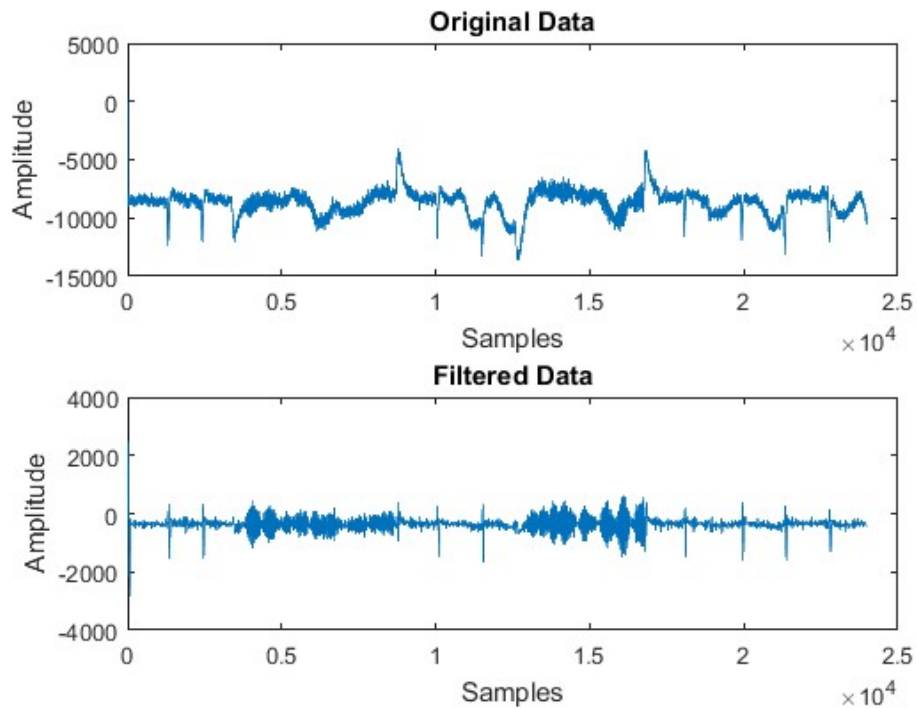


**Figure 39.** Filtering process.

The *RMS Envelope* was calculated by applying the following equation in a sliding window.

$$RMS = \left( \frac{1}{n} \sum_1^n f^2(n) \right)^{1/2}$$

**Where:**

**RMS** = Output Envelope,

**n** = number of sampled taken(window).

**f** = sampled values.

The window typically is moved one by one over the set of samples. The selection of  $n$  can be critical, since it will determine the smoothness of the output. A trade of in between large and small values also is required, like in the case of the filter, since the computation time will increase when the window is larger.

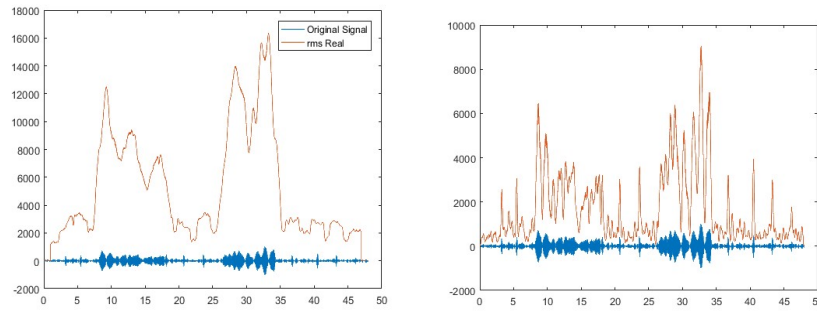


Figure 40. Smoothing of the envelope using different values of the window.

Summarizing the process, in the following figure is possible to see all the component mentioned before in flowchart of the scrip used on Matlab:

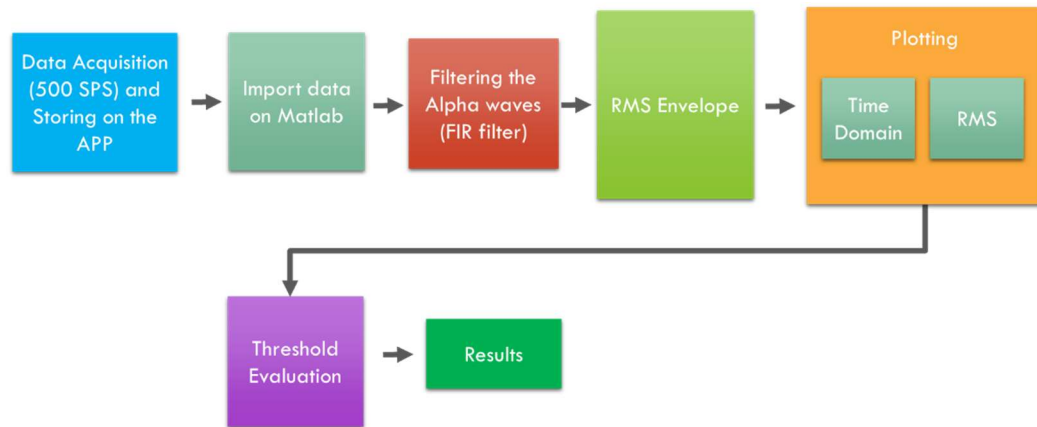


Figure 41. Envelope approach algorithm flowchart.

The selection of the threshold, as the same as in the previous case, was done by investigating the values of sensitivity and specificity in a normalized signal. The results are shown in the following table.

Method	Threshold Value	Sens	Spec	Score
Envelope RMS	0.4	0.935	0.925	0.861
Envelope RMS	0.425	0.801	0.958	0.76

Table 4. Envelope threshold comparison.

As It can be seen, the value of the threshold ( $th$ ) according to the score criterion that gives the best result is the one corresponding to the **threshold of 0.4**. The values were achieved by using the parameters for filtering and RMS detailed on the table 5.

Parameter	Value
Sample Frequency (Hz)	500
Filter order (Alpha band)	100
Window Size (RMS)	500

Table 5. Envelope threshold comparison.

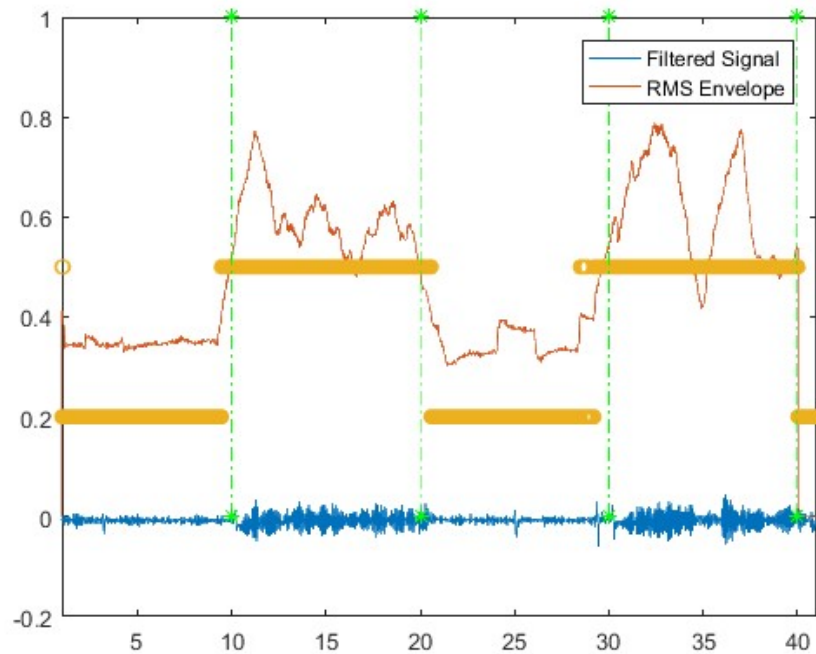
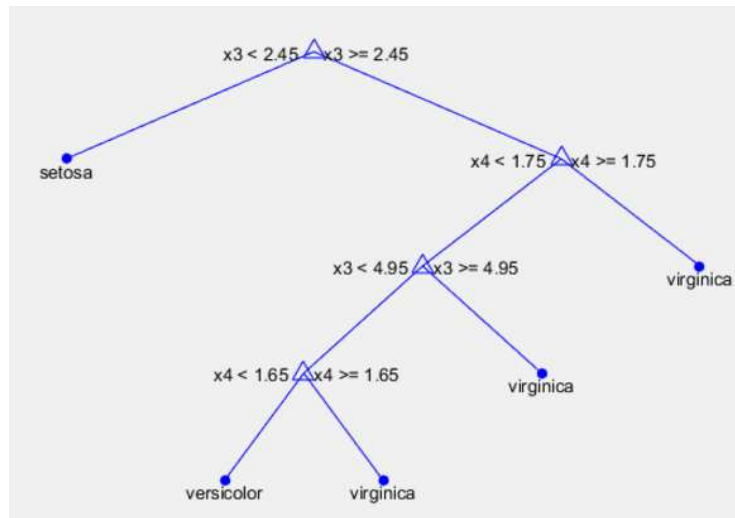


Figure 42. One trial with Threshold using an Envelope approach.

## 5.4 Decision Tree based approaches.

These methods correspond to the evaluation of the signal by using time-series features like average, standard deviation, min, max and range. A feature extraction of the signal is performed in the two different distinguishable Classes, Eyes opened and Eyes Closed. While the decision tree is running, the parameters of these two classes are compared with real time measurement to obtain the outputs.



**Figure 43.** Decision Tree example.

Also, it was tested the use of PSD values as features of the classes with the time-series features. Likewise, it was investigated the viability of detecting the blink of the eye as a new class. The following models were tested:

**5.4.1 Binary Decision Tree:** In this case, the classes were characterized by using only the typical features for time-series classification. Some sections of the trials were selected as training data. Initially the cross-validation (5 folds) gave good results for the simple tree. However, the results with the real trials showed that the medium tree (more complex) was slightly more suitable for this implementation. The results are the following:

Method	Tree	Spec	Sens	Score
DT	Simple	0.790	0.887	0.678
DT	Medium	0.828	0.855	0.683

Table 6. Binary decision tree model comparison.

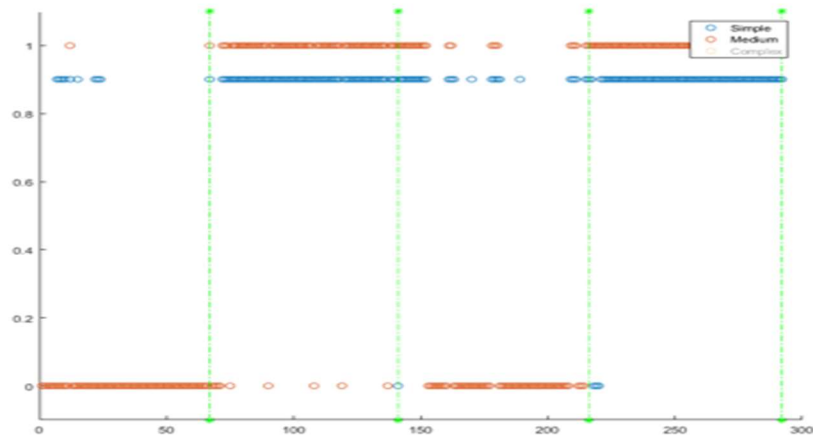


Figure 44. Binary decision tree predictions

After some experimentation, it was found that it was possible to increase the performance (or keep it the same) just by avoiding the use of some features. This is important since it will allow decrease the processing time of the decision tree algorithm. The results conclude that Is slightly better just to take the Average and Standard Deviation (Medium tree).

Method	Details	Sens	Spec	Score
DT(medium)	AVG+RG	0.839	0.718	0.557
DT(medium)	AVG+STD	0.885	0.789	0.674
DT(medium)	STD+RG	0.834	0.834	0.668

Table 7. Binary decision tree eliminating some features.



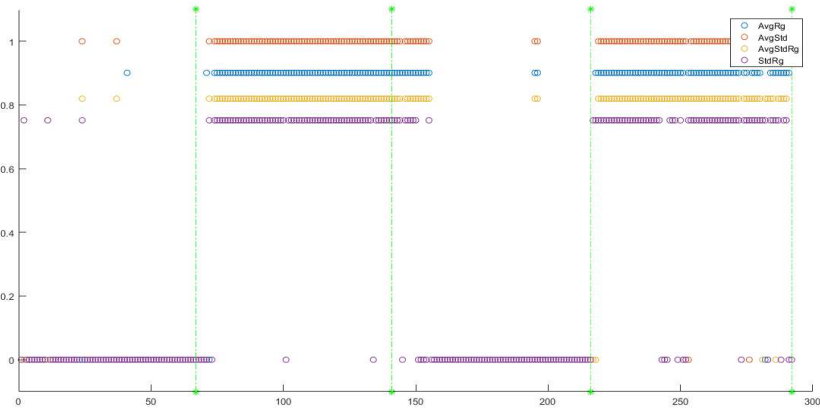


Figure 45. Binary decision tree predictions after eliminating some features.

**5.4.2 Binary Decision Tree including the PSD as a feature:** In this case, the same approach has been taken but also adding a normalized version of the PSD as a new feature. It was also included the theta band with the aim to eliminate the interference caused by the blinks (as introduced on chapter 2). Different combinations of these features were tested, and the results are shown in the following table.

Method	Tree Feat	Sens	Spec	Score
DT	AVG+SV+Aw+Tw	0.945	0.888	0.843
DT	AVG+SV+Aw	0.932	0.843	0.776
DT	AVG+SV +Tw	0.819	0.859	0.679

Table 8. Decision tree with PSD model comparison.

**5.4.3 3-Ary Decision Tree:** Targeting the detection of the blinks, the system has been trained with the aim to detect the blinks, the results are the following (based in the confusion matrix).

Method	Details(Features)	Popen	Pclose	Pblink
Simple	All Features	0.655	0.889	0.621
Medium	All Features	0.603	0.858	0.608
Simple	AVG+STd+Pws	0.625	0.889	0.660
Medium	AVG+STd+Pws	0.572	0.855	0.647

Table 9. 3-ary Decision tree with PSD model comparison using blink as a new class.

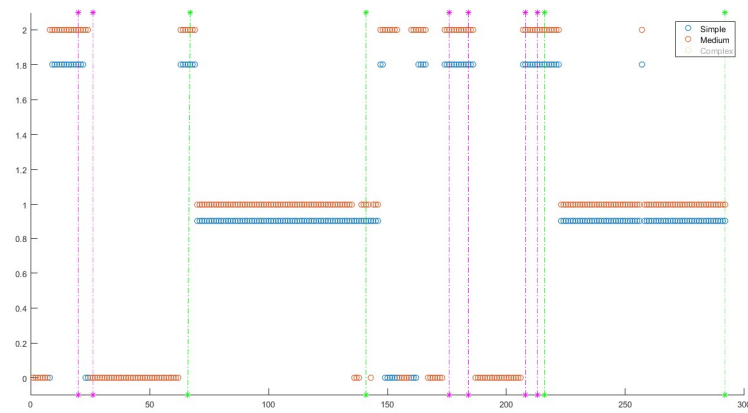


Figure 46. 3-ary Decision tree with PSD model prediction using blink as a new class.

**5.4.4 Blink trained as ‘open eyes’:** Since the detection of the blink was interfering with the other parameters, and at the same time was not correctly detected by the method reported before, this feature was used as training data for ‘eyes open’ class. The results can be seen in the following table.

Method	Details	Sens	Spec	Score
DT(Simple)	Blink as Open	0.860	0.961	0.822
DT(Medium)	Blink as Open	0.857	0.957	0.815

Table 10. Decision tree with Blink as Open eyes.

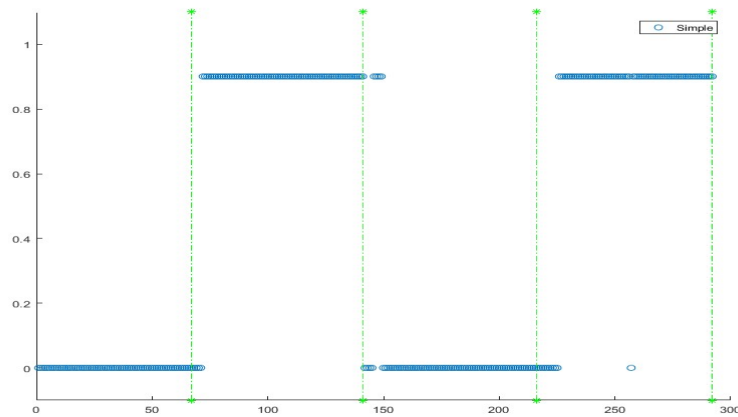
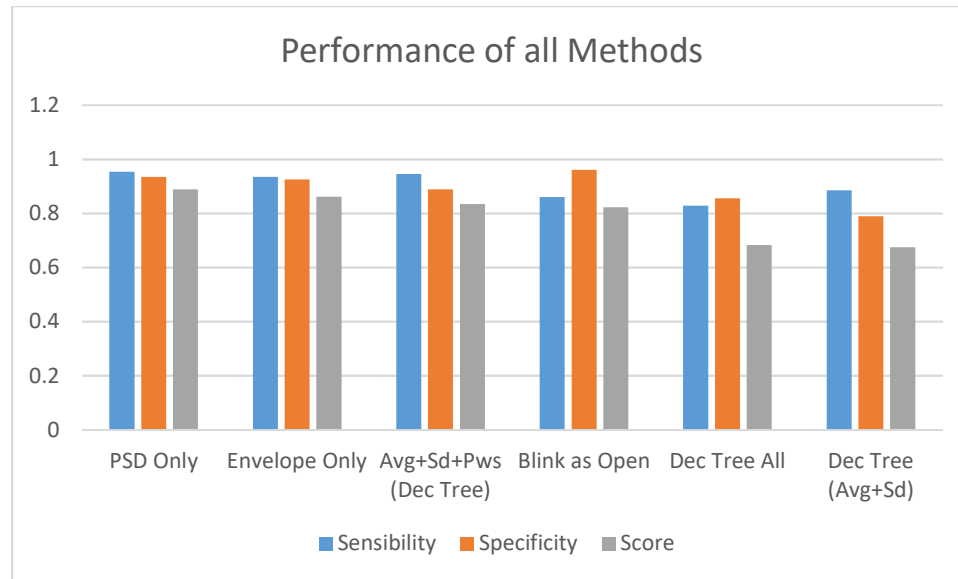


Figure 47. Blink trained as ‘open eyes’ model prediction.

## 5.5 Data analysis and selection of the final Implementation.

The purpose of this exploratory analysis was to determine which of the methods will be more suitable for the final implementation. After evaluation the different parameters and considering the computational power and complexity as factor of choice, the threshold approaches have shown remarkable performance. Nevertheless, the decision three using PSD as feature also show good results but the computational complexity for this case is higher, which make it less viable for a final implementation.



**Figure 48.** Performance graph.

In the figure is possible to see all the methods organized by the value of the score, the PSD and Envelope approaches have almost the same performance, followed by the Decision tree with the PSD's as features. The values for the 3-ary decision tree are not shown since they fall behind expected performance.

The threshold methods in theory will not require any training, apart from some tuning, which is always part of any kind of final implementation, particularly in this case, since the exploration was done with offline data and the requirement for this project force an online solution.

The PSD method show a small advantage (about 2.7% more) over the envelope method. However, it will require more DSP instructions, since it will be required a DC offset Filter, a Notch Filter and the calculation of the PSD on itself. We believe that for that reason, the envelope approach represents an easier solution since its implementation will require just one filter and then the calculation of the RMS Envelope

This gave us the motivation to choose this method for the final implementation on the microcontroller. The general block diagram for this process can be seen at the next figure.



*Figure 49. Final model.*

As stated before, the decision tree method with PSD and also the threshold detector using PSD have good potential, but this project will leave the testing of these implementations for a future work.

## **6 Implementation of the model and experimental results.**

The analysis of the data proposed on the previous chapter has an offline prospective. All the code was developed taking into account the existence of the dataset. For that reason, some changes have been made on the code while translating the MATLAB scrips to a given language. The C based OpenSTM32 IDE was used for programming the microcontroller. It's a software based on eclipse and allows the debugging of the board.

In this chapter, this process will be explained as the same as the experimental results regarding the detection of the alpha waves while utilizing the device on real time and implementing the envelope approach.

### **6.5 Translating the code to C.**

The main part of the firmware used for the acquisition of the data from the AFE was kept as the same as the initial version. Particular modifications are related to the inclusion of the DSP algorithms in order to implement the envelope approach.

Luckily, there exist a series of libraries for DSP available for ARM processors, called CMSIS, that can be used for the computations required by the model created in Matlab. They are well known algorithms optimized for a single cycle execution, very important parameter while dealing with real time applications.

The CMSIS enables consistent and simple software interfaces to the processor for interface peripherals, real-time operating systems, and middleware. It simplifies software re-use, reducing the learning curve for new microcontroller developers and cutting the time-to-market for devices [24].

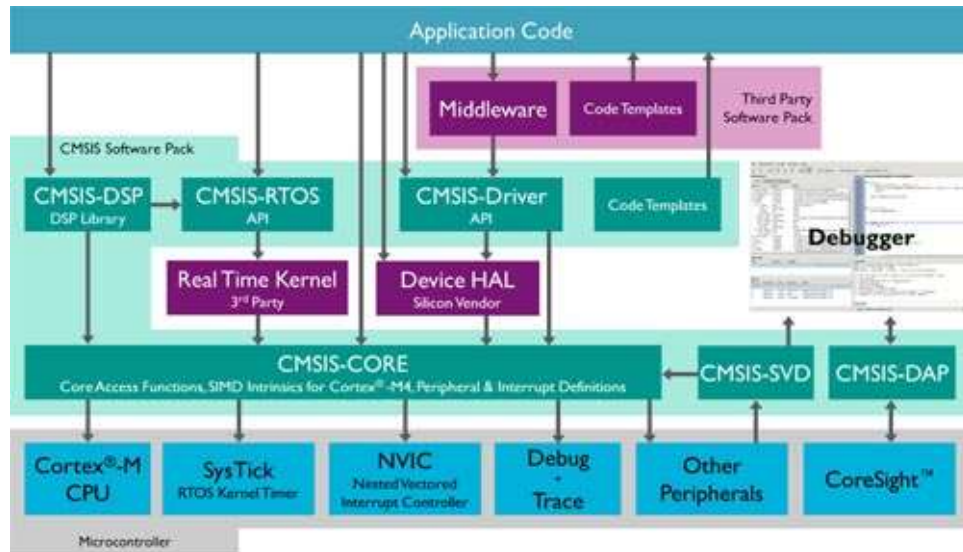


Figure 50. CMSIS Library Scheme [24].

It contains several modules, The CMSIS-Core, The CMSIS-DSP, CMSIS-RTOS, CMSIS-SVD, and others. During the work, only the module of CMSIS-DSP was used. This module is a collection of 60 Functions for DSP.

The following DSP libraries were used for the envelope approach:

- **ARM\_FIR\_Filtering:** used to band pass only the signals that belong to the Alpha wave frequency band. This function will accept a structure containing the parameter of the filter (\*S), a pointer to the input signal (\*pSrc), a pointer to the output (\*pDst) and a constant with the block size (blockSize).

*arm\_fir\_xxx (const \* S,\* pSrc,\* pDst, blockSize )*

- **ARM\_RMS\_ENVELOPE:** This library will extract the envelope of the filtered signals using the Root Mean Square technique. It requires as input a pointer to the source data (\*pSrc), a constant indicating the block size (blockSize) and a pointer to the output (\*pResult).

*arm\_rms\_xxx (\* pSrc, blockSize,\* pResult )*

**Obs:** the \_xxx letters stand for the different datatypes that the functions can assume.

Since the data is processed in blocks in the DSP, a circular buffer was added in order to preserve the structure of the data.

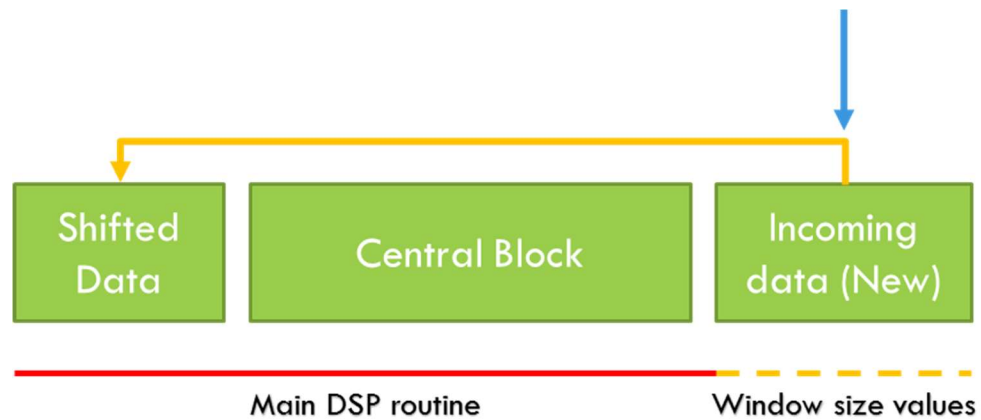


Figure 51. Circular Buffer.

## 6.6 Other adaptations of the code.

During the experimentation, some changes were added in order eliminate the blink of the eyes and a new phenomenon that was observed. This is related to the fact that not always the alpha waves are constant. i.e., they may vary in amplitude.

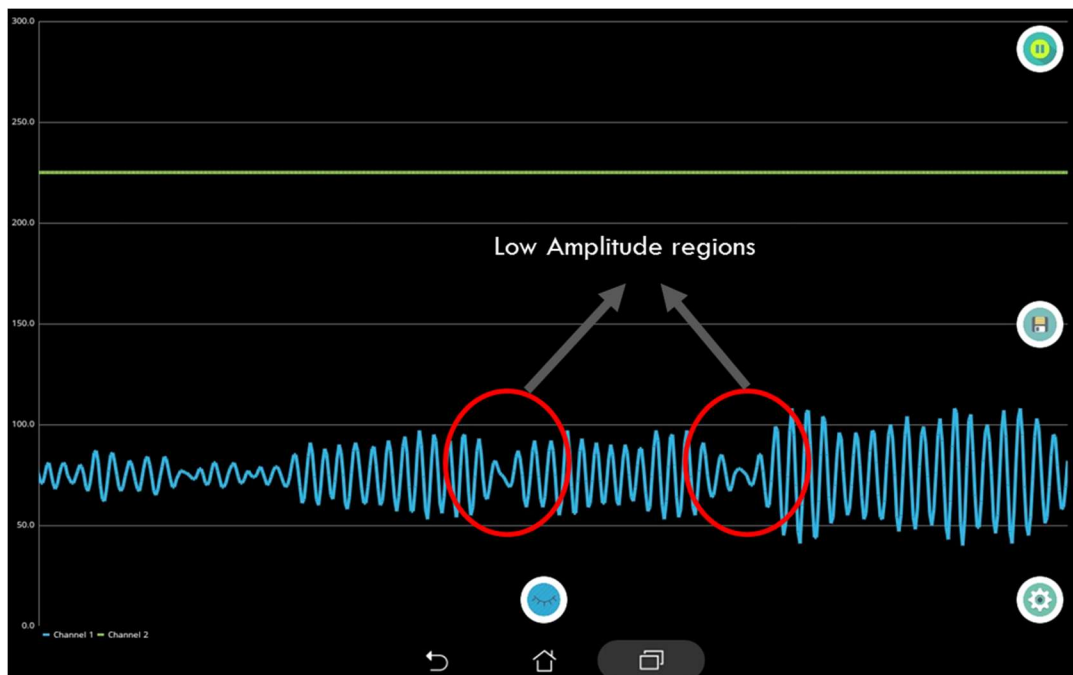


Figure 52. Decrease of the Alpha waves signal amplitude.

- **Low pass filter:** In order to eliminate the fast transitions generated by the blink of the eye, a low pass filter applied to the predictor algorithm was applied. The algorithm uses the following commands.

The value of filter ( $\alpha$ , see the algorithm bellow) was determined by selecting the value that generates the lower error. Also, this algorithm was useful in order to stabilize the traitorous values that may appear making the Prediction smoother.

- **Dynamic Thresholding:** this method will allow to decrease the threshold while the prediction is Closed eyes, favoring the correct detection when there are some variations on the energy of the alpha waves (see figure 52). The threshold will change if the value of  $\beta$  is reached.

Both adaptations are controlled by the following algorithm:

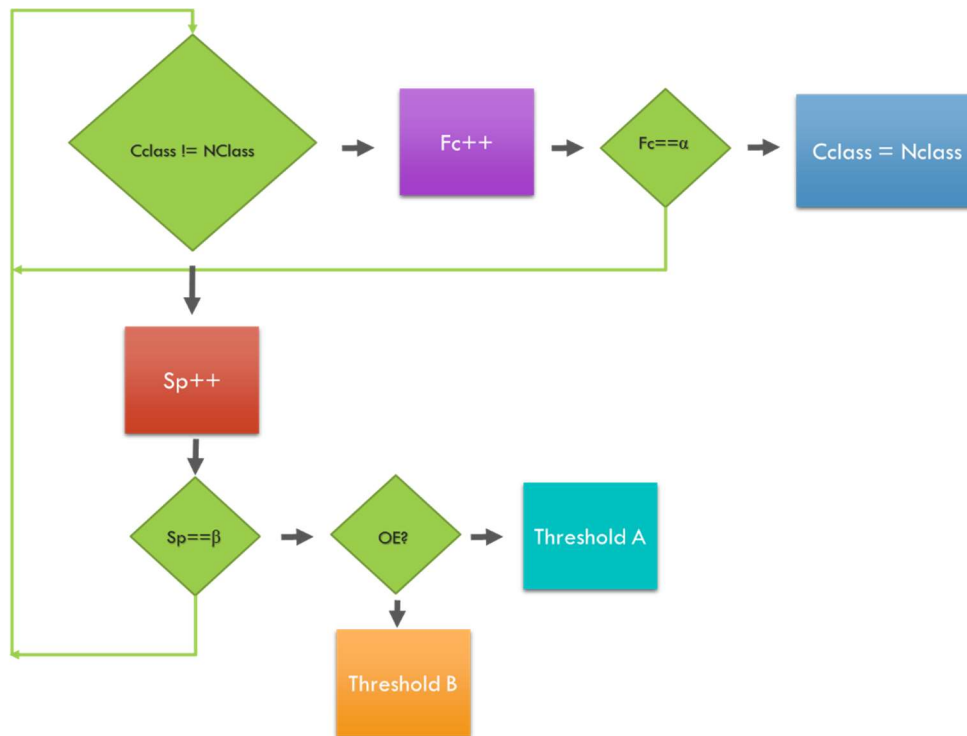


**Figure 53.** Algorithm used for the adaptations.



Where:

**CClass** = Current Class

**Fc** = Filter Counter.

**Sp** = same prediction counter.

**OE** = Open Eyes.

$\alpha$  = Filter value.

$\beta$  = minimum number of same predictions for changing the threshold.

## 6.7 Testing Setup.

The final device, with the firmware included the DSP routines were tested with three test subjects. The same cares that when taking the initial readings were taken. For this, the testing application detailed on the chapter 4, section 3 was used. In the following figure is possible to see the whole implementation in one of the test subjects.

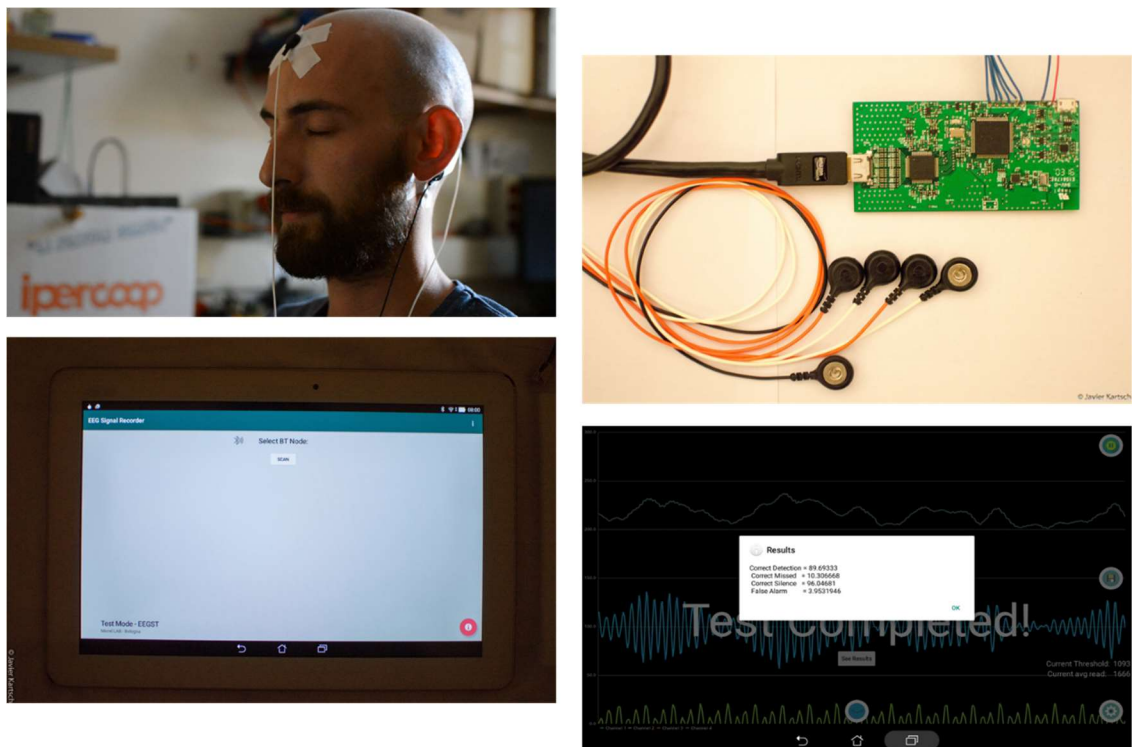


Figure 54. Test phase

## 6.8 Results.

Following the same procedure for the acquisition of data from the subject on the chapter 5, section 1, and using the Android test tool detailed on the chapter 4, section 3 it was possible to obtain the following results while using the Envelope approach:

- **Sensitivity** = 0.882
- **Specificity** = 0.934.
- **Score** = 0.881.

Taking in consideration the values from the MATLAB modeling, the final implementation was able to predict almost with the same accuracy the respective classes. Some final tune up was done on the system at the end. The value of the window of the RMS was changed to 225 samples in order to accelerate the processing velocity with no degradation of the performance. The order of the Alpha band filter was kept the same. The prediction time was finally in between 1 and 5ms.

Despite the fact that this work didn't targeted the energy consumption of the board is important to mention that the consumed power, in average was of the order of the 250 mW, a parameter to be improved in future implementations.

The following figure show the system while extracting the envelope and making the threshold decision.

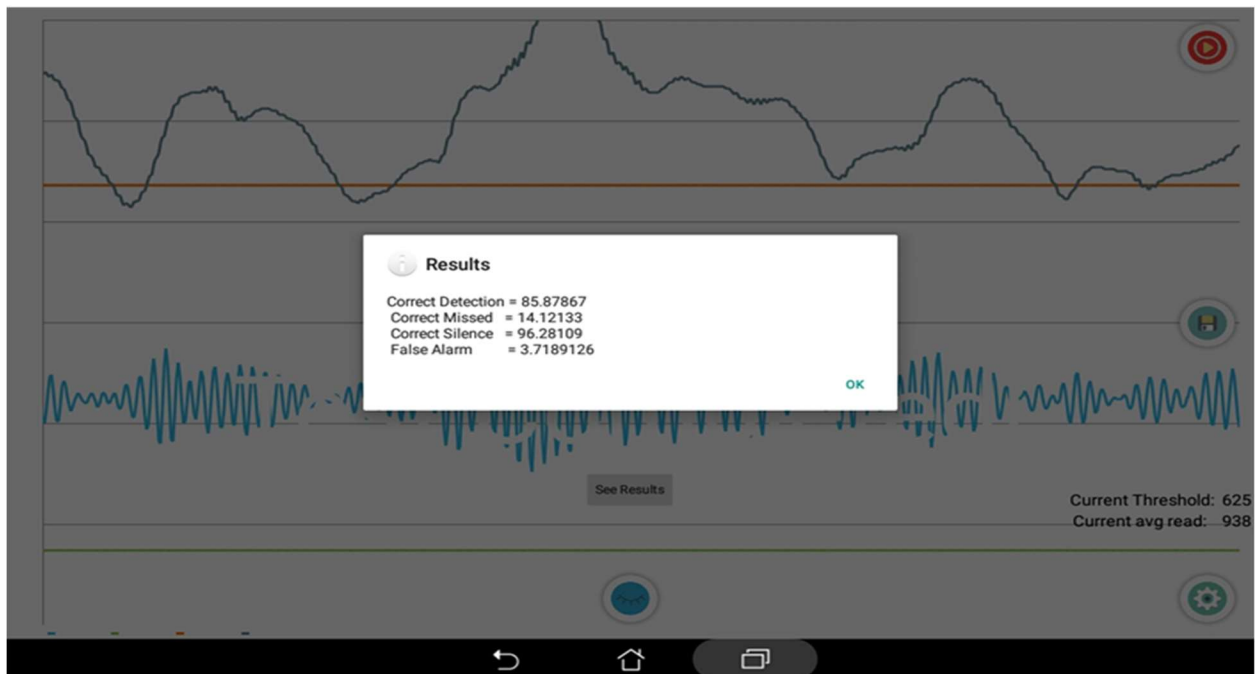
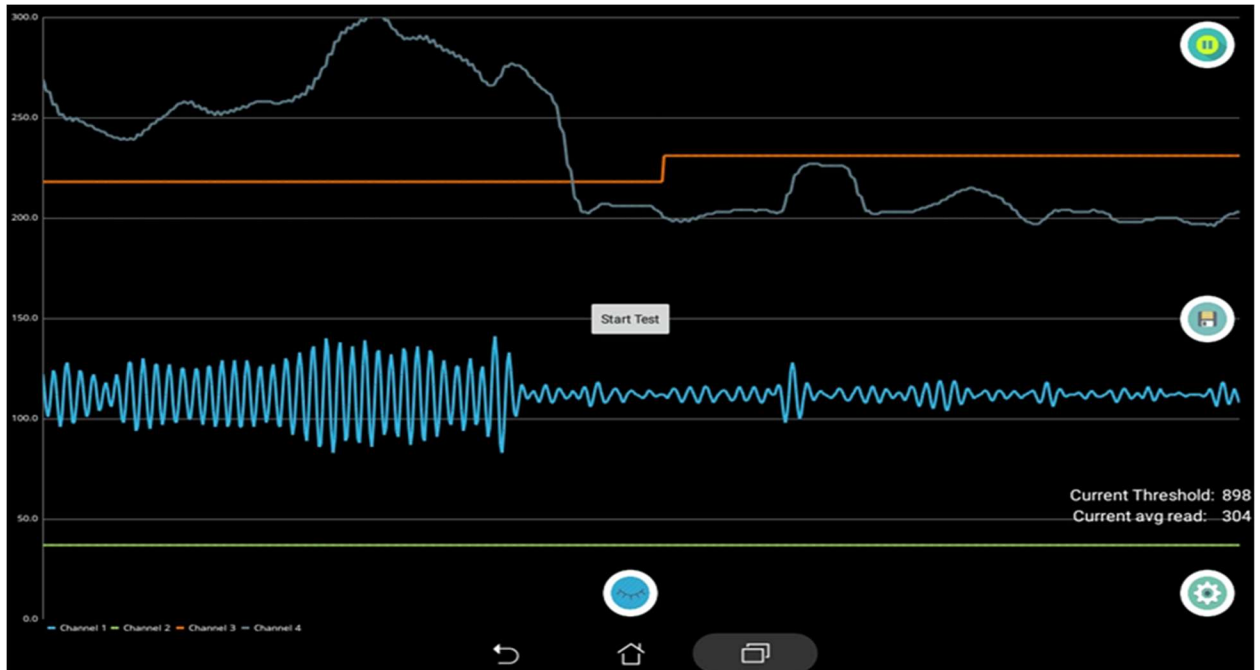


Figure 55. Testing application showing test process and results.

## 7 Conclusions.

The development of software-hardware solutions with embedded systems present some advantages nowadays. Thanks to the new generation of boards and low power processors is possible to execute complex algorithms in a short time and we can start leaving the bulky computers towards a full portability. This have a huge impact on medical and monitoring applications. Currently is possible to acquire information from almost any kind of signal with increasingly fast systems. Nevertheless, the EEG signals have attached some extra challenges that we carefully were sorting during the development of this Online software-hardware embedded system.

Our implementation for detection the eyelid closure proved to the sufficiently accurate to be considered as another way for detecting this event, avoiding with it the inconvenient that the other implementations may have. With this is possible to have more information about the state of the user, and with this, avoid risky situations that can cause the loss of life, injuries, and material damage.

This implementation can be also combined with others using the same board while scanning other parameters since it can read other type of signals. This will permit the extraction of information in a single device that will generate more biomedical information for the user.

Still, this project will require additional research to become more robust. We based the selection of the envelope approach aiming a simple implementation, but other models have to be tested to determine how they will perform in comparison with the present implementation since working with offline data not always cover all randomness of the signals. Also some more testing is required to evaluate the performance in different environmental conditions that can affect, particularly, the AFE.

Knowing that wearable and implantable electronics can provide an improvement on the quality of life of the people, an effort on this area has always a tremendous impact. Even with small changes it's possible to reduce the number of accidents on the road or in industrial environments. Keeping this on mind, this project has encountered its motivation and also the desire of continuity.

## **Acknowledgements**

Special thanks to Prof. Luca Benini for giving me the opportunity work on this project. Also, to Dr. Simone Benatti, for his direct selfless support, day by day, for the corrections and suggestions to make this project a better work.

To my parents that in some way help me to be here now.

To the ERASMUS MUNDUS program, for giving me the chance to finish my studies at this university.

To the professors, staff, and colleagues of the University of Bologna as the same as my Home University, The National University of Itapua for opening the doors for a better education.

To all my friends for supporting me at the hard and also good moments during my stay in Italy.

And to my Oma, Herna Brehn de Kartsch, that was guiding me from above and also through my memories.

## References.

- [1] Caterpillar US, "Fatigue and Distraction Management", site: [http://www.cat.com/en\\_US/support/operations/technology/cat-minestar/detect/fatigue-management.html](http://www.cat.com/en_US/support/operations/technology/cat-minestar/detect/fatigue-management.html)
- [2] Mercedes Benz Ind, "Safety, Attention Assist", site: <https://www.mbusa.com/mercedes/benz/safety#module-3>
- [3] Fraunhofer IDMT, "Micro-Sleep Alert and Eyetracker", Fraunhofer Institute for Digital Media Technology, site: [http://www.idmt.fraunhofer.de/en/Press\\_and\\_Media/press\\_releases/2015/micro\\_sleep\\_alerter.html](http://www.idmt.fraunhofer.de/en/Press_and_Media/press_releases/2015/micro_sleep_alerter.html).
- [4] Smarteye Company, "Anti-sleep specifications", site: <http://smarteye.se/wp-content/uploads/2016/04/Anti-Sleep.pdf>.
- [5] S. Benatti; F. Casamassima; B. Milosevic; E. Farella; P. Schönle; T. Burger; Q. Huang; L. Benini, "A Versatile Embedded Platform for EMG Acquisition and Gesture Recognition", Micrel Lab – University of Bologna, Italy, IEEE, 2015.
- [6] Interaxon Company, "Muse Neuro Feedback specs", site = <http://www.choosemuse.com/>.
- [7] OpenBCI Alpha Wave Detector Project, site: <http://eeghacker.blogspot.it/2014/10/first-alpha-with-openbci-v3.html>
- [8] Li-Qun Zhang, Ph.D, "BME 366 Virtual Labs, Generation of the EMG", Northwestern University, site: <http://smpp.northwestern.edu/bmec66/weightlifting/emgback.html>.
- [9] Myo Control System, site: <https://www.myo.com/>
- [10] Anthony Atkielski, "Schematic Diagram of normal sinus rhythm for human heart as seen on ECG", January 2007.
- [11] Piotr W. Mirowski; Yann LeCun; Deepak Madhavan; Ruben Kuzniecky, "Comparing VM and Convolutional Networks for Epileptic Seizure Prediction from Intracranial EEG", 2016.
- [12] Tatum, W. O; Husain, A. M; Benbadis, S. R. "Electroencephalography, Handbook of EEG Interpretation", Demos Medical Publishing, 2007.
- [13] NeuroSky, "Multi-Channel EEG (BCI) Devices", site: <http://neurosky.com/2015/07/multi-channel-eeg-bci-devices/>
- [14] Medtronic, "Electrodes for EEG/EMG/ECG", site: <http://www.medtronic.com/covidien>
- [15] H. Nolan; R. Whelan, "Faster: Fully Automated Statistical Thresholding for EEG artifact Rejection", Trinity Center for Bioengineering, Trinity College Dublin, July 2010.
- [16] Whitham, Emma M; Pope, Kenneth J; Fitzgibbon, Sean P; Lewis, Trent W; Clark, C Richard; Loveless, Stephen; Broberg, Marita; Wallace, Angus; DeLosAngeles, Dylan; Lillie, Peter, "Scalp electrical recording during paralysis: Quantitative evidence that EEG frequencies above 20Hz are contaminated by EMG". Clinical Neurophysiology. Elsevier.
- [17] Andrii Cherninskyi, "The samples of main features of artifacts in Human EEG", October 2015.

- [18] American Clinical Neurophysiology Society, "Guideline 8: Guidelines for Recording Clinical EEG in Digital Media" Sample rates on EEG.
- [19] Texas Instruments, "Medical AFEs, ADS1298: Complete family of Analog Front Ends for EEG/EMG" site: <http://www.ti.com/lscds/ti/data-converters/precision-adc-less-10msps-medical-afes.page>.
- [20] STMicroelectronics, "STM32F407VG, High performance foundation line, ARM Cortex-M4 core with DSP and FPU, 1 Mbyte Flash, 168Mhz CPU, ART accelerator, Ethernet, FSMC Datasheet", September 2016.
- [21] Pjilipp Jahoda, "MPAndroid Chart, A powerful chart library for Android", 2016.
- [22] Hristo Zhivomirov, "Short- Time Fourier Transform (STFT) with Matlab Implementation", Matlab File Exange Program, August 2015.
- [23] Widmann A.; Schroger E.; Maess B., "Digital filter design for electrophysiological data – a practical approach", Cognitive and Viological Psychology, University of Leipzig and Max Planck Institute for Human Cognitive and Brain Sciences, Leipzig, Germany, August 2014.
- [24] ARM Consortium, "CMSIS – Cortex Microcontroller Software Interface Standard", site: <http://www.arm.com/products/processors/cortex-m/cortex-microcontroller-software-interface-standard.php>